

"It was cold in Missoula that day, and he came at me from nowhere with a Belt Argillite to identify. Quickly I grabbed my trusty rock identifier, and to my dismay, found it wanting."

*ANONYMOUS* (from 'Basics .. Sedimentology' by Fritz and Moore)

## CHAPTER 6 MINERALOGY AND PETROGRAPHY

### GENERAL

This chapter is aimed at furnishing the mineralogy in Lower Gondwana sediments and at examining the diagenetic changes that had taken place in them. Representative samples of shale and clay which form a secondary (except Talchir) but nevertheless an important part of the Gondwana sediments have been analysed for X-ray diffraction.

The results of all these analyses were utilized to ascertain the physical and chemical conditions of burial and to bring out the intrabasinal climate and tectonism operating during the Lower Gondwana sedimentation.

### TALCHIR FORMATION

The Talchir Formation consists of diamictites, shales, and sandstones. Megascopic characters of these rock units have already been discussed in Chapter-1. The textural and mineralogical characters of Talchir Formation, as revealed from thin-section studies have therefore, been discussed here in detail.

Under microscope, the Talchir sandstones exhibit fragmental texture consisting of quartz (56.6 %), feldspar (3.39 %), unstable lithic fragments (4.23 %) and garnets (1.26 %) as framework particles. These are embedded in matrix which is dominantly chloritic in nature (Plate 6.1). The matrix constitutes about 35 to 45 % by volume of the framework. The particles show poor sorting with sizes ranging from 0.1 mm to 3 mm. The quartz and feldspar grains are sub-angular to sub-rounded, while the rock fragments show more sub-rounded outline. Compaction is poor and the grains show floating contacts.

Within quartz, monocrystalline varieties (55.87 %) dominate over the polycrystalline ones. Undulatory quartz accounts for 2.12 % of the monocrystalline variety. Feldspars observed are mainly plagioclase with subordinate K-feldspars (orthoclase, microcline). Perthites are not uncommon.

**Plate 6.1-6.5 Photomicrographs of Talchir Sandstones**

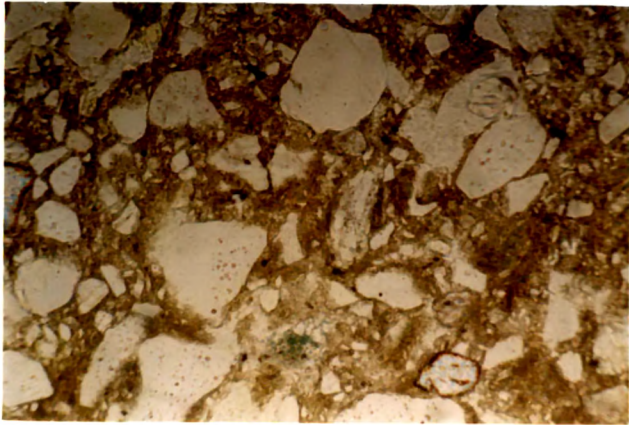
**Plate 6.1 Chlorite matrix. (40X; PPL)**

**Plate 6.2 Sedimentary rock fragments of limestone and cherty siltstone. (40X; Crossed Nicol)**

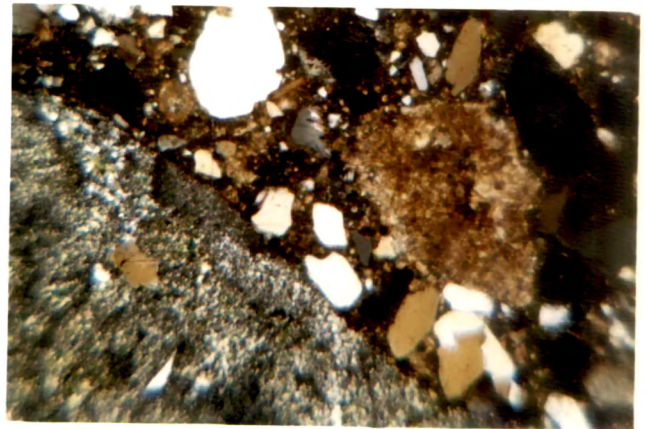
**Plate 6.3 Alteration (depth controlled) of plagioclase into illite (?). (75X; Crossed Nicol)**

**Plate 6.4 Late stage replacement of chlorite matrix by calcite. (40X; Crossed Nicol)**

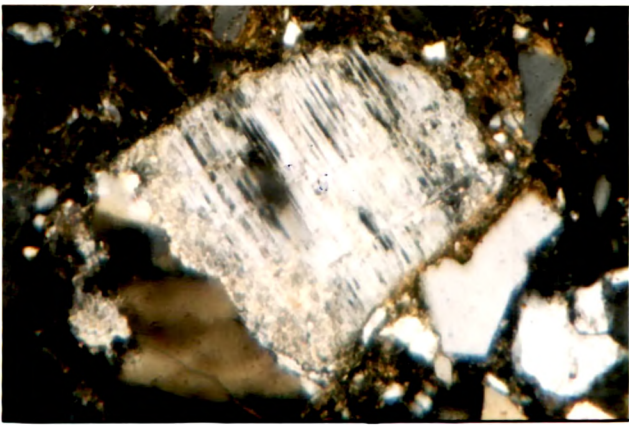
**Plate 6.5 Development of syntaxial calcite rim around limestone fragment. (75X; Crossed Nicol)**



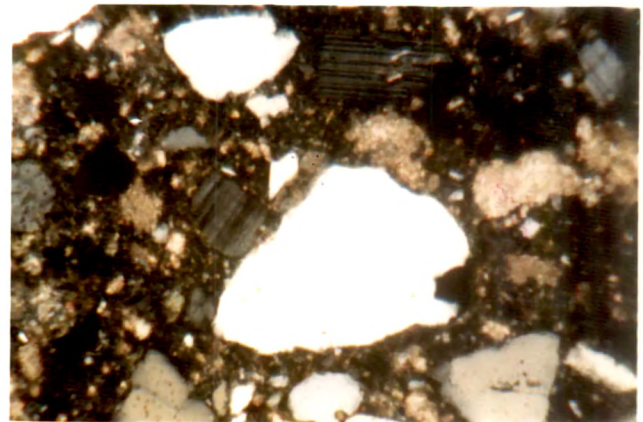
6.1



6.2



6.3



6.4



6.5

Within the unstable lithic fragments, sedimentary rock fragments such as limestones, sandstones and siltstones are observed to be dominating (Plate 6.2). Besides these, fragments of mica-granites and gneisses have also been observed. Garnets are found to be the most common accessory mineral.

Based on the percentages of framework particles and matrix, sandstones of Talchir Formation can be classified as 'Arkosic wacke' (Dott, 1964).

## **DIAGENESIS**

The sandstones of Talchir Formation are characterised by prominent mineral replacement that resulted in lithification and thus can be said to exhibit locomorphic stage of clastic diagenesis (Dapples 1985).

The matrix, dominantly chloritic, constitutes 35-40 % by volume of the rock. It is clearly observed that these chlorites were recrystallized from the detrital clay pointing to the authigenic origin of the matrix. Following Dickinson (1970) this may be termed as orthomatrix. At places the recrystallization is so complete that the interstitial chlorites appear more as cement (phyllosilicate cement of Dickinson, 1970). These authigenic chlorites were possibly derived from the fixation of cations, released through the early dissolution of ferro-magnesium minerals during the times of aridity. Tardy (1971) has shown that meteoric water with high ionic activity is characteristic of arid climates. Indeed, climate during the Talchir time was cold and semiarid (Casshyap and Qidwai, 1974; Bose and Ramanamurthy, 1979; Suttner and Dutta, 1986; Soman and Kale, 1993). Thus the climate-controlled groundwater chemistry played fairly important part in the authigenesis of chlorite in Talchir sandstones. The near absence of Biotite (which otherwise is a characteristic mineral of reducing, deep burial diagenetic environment) within the Talchir sandstones further testifies the importance of role of climate in the first stage of authigenesis.

The role of burial diagenesis within the Talchir sandstones, however, cannot be altogether ruled out. Presence of feldspars showing full and/or partial alterations are frequently observed (Plate 6.3). These alterations are not controlled by provenance or distance of transport but by the depth of burial. Decomposition of feldspar into kaolinite requires a humid climate (Folk,

1968) whereas illitization of feldspars is depth and temperature controlled (Keller, 1970). Since the climate during the Talchir time was semi arid and the ground water chemistry was also not conclusive to the formation of kaolinite, the author considers that the alteration of detrital feldspars is in essence, a process of illitization which was augmented by a deep burial condition (maximum of about 3500 metres) and a temperature in the range of 130°-140°C (assuming a mean surface temperature of 20°C and world geothermal gradient of 1°C/30 m). This conforms to the findings of Maxell (1964) who reported the process of illitization to start at a depth of 2000 m where the geothermal temperature range is 40-116°C.

The chlorite matrix/(and or cement?), at places shows replacement by calcite (Plate 6.4). The replacement is not total and interstitial chlorite matrix are disbursed within the calcite. Such changes are observed in local stratigraphic positions, particularly at sites of lateral or vertical proximity to limestones. Presence of abundant fragments of limestone within the Talchir sands corroborates the fact that the site of Talchir sedimentation was very near to pre-existing limestone deposits (Pakhal Formation). At places, the limestone fragments show development of syntaxial calcite rim (Plate 6.5) which may be ascribed to being deposited from interstitial solution of high pH on to the free surface of the rock fragment (Bathurst 1958).

Thus diagenetically, the Talchir sandstones represent two distinct stages. The first stage is characterized by crystallization of chlorite, from detrital finer clastics and this change was influenced by climate controlled groundwater chemistry. Parameters such as depth, temperature and local variation in Eh-pH conditions were the controlling factors in the second stage during which the detrital feldspars were altered into illite and earlier formed chlorite was partially replaced by calcite.

## **BARAKAR FORMATION**

Barakar Formation consists predominantly of sandstones with subordinate shales, carbonaceous shales and coal seams.

The Barakar sandstones constitute 75-80 % by volume of the formation. In hand specimen it is coarse to medium grained, grey to greyish white in

colour on fresh surface, loosely cemented with occasional mica laminae and disseminated grains of garnet.

Under the microscope, the Barakar sandstones show fragmental texture and consist of 82 % framework particles and 18 % matrix. The grains are angular to sub-rounded and show moderate to poor sorting. Point and floating contacts are dominant. However, where matrix content is less than 10 %, the grains show long contact. Sutured and concavo-convex contacts are also seen in well compacted sandstones (Plate 6.6).

Since Barakar sandstones contain more than 5 % clay and the grains are, in general, poorly sorted and angular to sub-rounded, they can be termed as texturally immature (Folk, 1968). At few places, however, textural inversion (Folk, 1968) can be seen where well sorted sand grains are embedded in a clay matrix of over 5 % (Plate 6.6).

Quartz is one of the chief framework particles and constitutes 64.55 % by volume of the Barakar sandstones (Table 6.1). Of this, 62.36 % are monocrystalline and 2.19 % are polycrystalline quartz. Within the monocrystalline variety, 95.36 % are non-undulatory quartz. The next abundant framework grains are the feldspars. Orthoclase, microcline and perthites (Plate 6.7) are the most common. Na-plagioclase is present in lesser amounts. Together, they constitute 12.3 % by volume of the Barakar sandstones. Unstable lithic fragments are very rare and their amount is only 0.5 %. Micas (both detrital and authigenic) make up 4.19 % while the accessories, of which garnet is the most common, constitute 1.04 % of the Barakar sandstones.

Average matrix content in Barakar sandstones is 17.3 %. Matrix content within the sandstones varies erratically from one place/horizon to another and their range is from 8 % to 28 %. Matrix within the Barakar sandstone is argillaceous of which kaolinite is most predominant (Plate 6.8). At few places the matrix is chloritic in composition. Barakar sandstones, in general are poorly cemented. Cement is mainly calcareous.

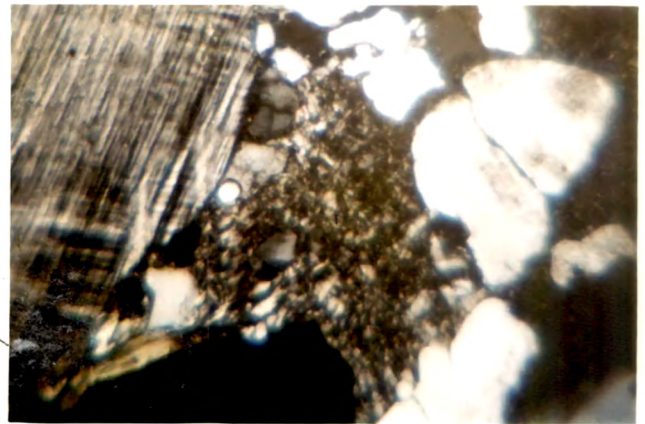
From the average percentage of particles (Quartz-64.55; Feldspar-12.29, Rock fragments -0.5 %) and matrix (17.3 %), the sandstones of Barakar Formation can be classified as sub-arkosic (or arkosic) wacke (Dott, 1964).

**Plate 6.6-6.10 Photomicrograph of Barakar Sandstones**

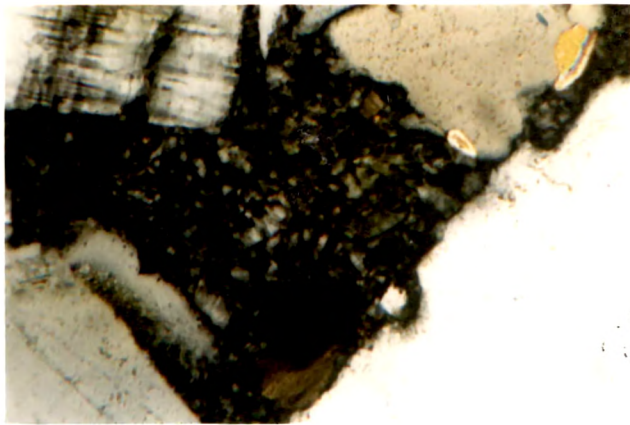
- Plate 6.6** Well compacted sandstone showing plane and saturated contacts between the framework grains. (40X; Crossed Nicol)
- Plate 6.7** Grain of perthite (left) and argillaceous matrix. (75X; Crossed Nicol)
- Plate 6.8** Pore filling kaolinite matrix. (75X; Crossed Nicol)
- Plate 6.9** Alteration of detrital K-feldspar (orthoclase) into kaolinite. (40X; Crossed Nicol)
- Plate 6.10** Alteration of plagioclase into smectite or illite (?) (75X; Crossed Nicol).



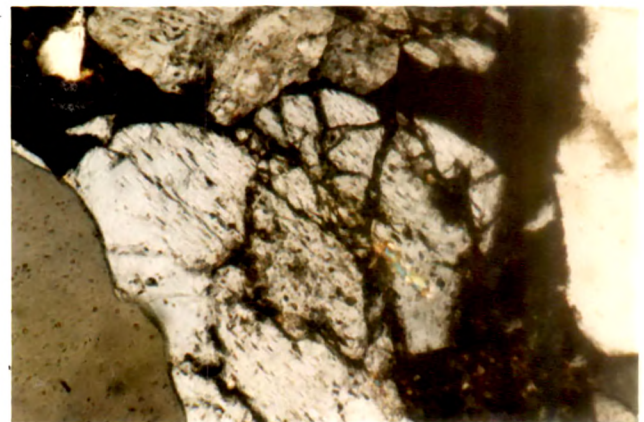
6.6



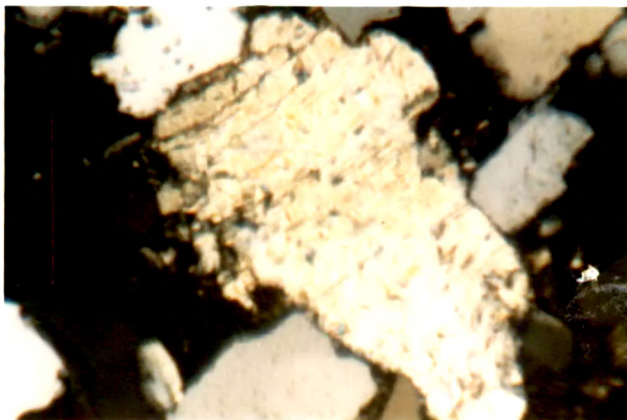
6.7



6.8



6.9



6.10

TABLE 6.1 : MODAL COMPOSITION OF BARAKAR SANDSTONES

Sample No.	Depth (m)	Q U A R T Z						Rock Fragments	Mica	Accessories	Matrix	Cement	Q:Rx
		Monocrystalline		Polycrystalline	Total	Feldspar	Mica						
		Non Undulose	Undulose										
B1/74	416.72	59.65	5.15	64.80	2.21	67.01	1.10	3.68	-	12	-	77:19:4	
B1/75	421.82	37.29	3.24	70.53	4.86	75.39	0.40	1.21	-	10	-	79:15:6	
B1/77	428.00	63.25	5.39	68.64	0.72	69.36	-	7.91	-	8	-	82:17:1	
B1/78	444.24	62.79	2.51	65.30	3.07	68.37	1.39	1.67	-	16	-	79:15:6	
B1/79	447.54	61.22	2.72	63.94	2.99	66.93	1.63	0.27	1.90	20	-	82:12:6	
B1/81	449.00	66.93	2.97	69.90	0.99	70.89	0.14	0.70	7.35	11	-	86:12:2	
B1/83	465.00	64.76	4.35	69.11	2.72	71.83	-	0.74	-	20	-	86:10:4	
B1/84	476.00	59.23	3.22	62.45	2.48	64.93	0.25	1.81	1.21	15	4	74:23:3	
B1/85	493.00	58.60	2.41	61.01	3.62	63.63	0.60	1.80	1.21	9	-	73:22:5	
B1/86	497.85	49.27	4.51	53.78	0.75	54.53	0.38	16.80	-	18	-	85:13:2	
B1/88	511.00	55.66	1.69	57.35	3.13	60.48	-	2.89	0.72	20	-	75:21:4	
B2/38	220.50	52.63	4.07	56.70	2.69	59.29	-	5.56	-	14	-	71:26:3	
B2/39	221.50	57.02	3.02	60.04	1.61	61.65	0.40	11.89	-	18	-	86:12:2	
B2/40	222.50	53.17	6.25	59.42	4.69	64.11	1.25	3.75	-	24	-	82:10:8	
B2/41	229.50	58.07	2.85	60.92	0.85	61.77	0.28	1.71	3.70	22	-	84:14:2	
B2/44	237.50	50.32	5.03	55.35	1.51	56.86	0.50	5.53	-	22	-	81:16:3	
B2/45	238.50	64.64	3.92	68.56	0.58	69.14	0.19	5.68	1.17	14	-	87:12:1	
B2/47	250.00	68.19	3.24	71.43	0.43	71.86	0.20	2.59	1.08	16	-	89:10:1	
B2/51	278.00	69.62	1.29	70.91	1.54	72.45	-	4.64	3.61	10	-	87:11:2	
B2/59	287.50	52.10	4.53	56.63	4.07	60.70	-	4.98	-	18	-	74:21:5	
B2/60	290.00	61.98	2.58	64.56	2.32	66.88	-	2.84	-	14	-	85:12:3	
B2/61	293.50	47.13	1.64	48.77	1.84	50.61	-	11.47	-	25	-	77:20:3	
B2/62	294.50	61.34	1.34	62.68	0.50	63.18	1.01	3.36	3.19	3	17	85:13:2	
B2/64	300.00	64.40	1.40	65.80	0.46	66.26	0.46	9.62	3.26	12	-	88:11:1	
B2/67	306.50	58.62	-	58.62	1.14	59.76	-	3.41	1.14	-	30	89:9:2	
B2/68	312.50	52.73	5.07	57.80	1.01	58.81	-	-	-	28	-	80:18:2	
B2/76	334.50	57.31	2.24	59.55	1.74	61.29	0.75	1.49	1.00	24	-	81:17:2	
B2/77	337.50	57.18	1.14	58.32	1.90	60.22	0.19	4.00	1.33	23	-	81:16:3	
B2/83	352.50	62.63	1.47	64.10	3.68	67.78	0.74	1.47	-	16	-	78:17:5	
S2/84	355.00	58.76	0.87	59.63	4.35	63.98	0.43	1.74	-	16	-	72:22:6	
M1/63	498.00	68.09	2.35	70.44	0.59	71.03	0.88	2.64	1.76	14	-	86:12:2	
M1/64	504.00	62.96	4.29	67.25	1.91	69.16	-	0.47	0.47	17	-	82:16:2	
M1/65	525.00	52.14	1.43	53.57	5.00	58.57	2.14	14.28	-	10	-	71:20:9	
M1/67	561.00	62.49	-	62.49	3.68	66.17	1.22	-	-	10	3	72:22:6	

## **DIAGENESIS**

Barakar sandstones fall in Dott's (1964) wacke class with matrix constituting 17.3 % by volume of the rock. Changes in texture and composition of the matrix are the main features of the diagenetic environment of Barakar sandstones. The change was induced by two processes-first, reconstitution and recrystallisation of the detrital clay minerals into authigenic ones and second, alteration of detrital and early formed authigenic minerals into newer ones.

Kaolinite is the principal clay mineral that constitutes the matrix of Barakar sandstones and has imparted a predominant white to grey-white colour to it. The process of kaolinization of the matrix is due to weathering and breakdown of the detrital feldspar grains in a wet and humid climate, which, indeed, was prevailing during Barakar sedimentation (Folk, 1968). In Raniganj coal field, Dutta and Suttner (1986) correlated the abundance of kaolinite in Barakar sandstones of Damodar valley to extensive dilution of the pore water with respect to ferromagnesium ions that dominate the rocks of Lower Talchir Formation in the form of chlorite. Extensive dilution of pore water suggests substantial rainfall to have taken place. Thus precipitation of kaolinite in Barakar sandstones was controlled by climate which was essentially wet and humid during the Barakar time.

In Barakar sandstones kaolinite occurs mostly as pore-lining and pore-filling cement (Plate 6.8). Minor amounts occur as visible alteration of detrital feldspar (Plate 6.9). At few places plagioclase feldspars shows alteration into smectite (or illite ?) (Plate 6.10).

Although present in substantial quantity, feldspars are mostly partially weathered (Plate 6.9). Completely fresh feldspars are comparatively lesser whereas fully weathered (kaolinised) feldspars are rare. Folk (1968) and Pettijohn (1984) emphasized the importance of both climate and tectonic activity on the occurrence of feldspar in sandstone. According to their views, mixture of semi-altered and fresh feldspars in Barakar sandstones can be attributed to rapid erosion of an elevated rugged source area, rich in feldspars, in a climate lying somewhere between temperate humid to warm humid. Presence of some fresh feldspars suggests that sedimentation was

rapid, followed by quick burial, thereby not allowing the feldspars to atmospheric weathering.

Micas (4.19 %) in the Barakar sandstones are represented by both detrital and authigenic types. Biotite and muscovite are encountered both as authigenic and detrital variety whereas chlorite is fully authigenic. The alteration of one mica into another was mainly brought about by the existing Eh conditions which, from the assemblages of micas, seemed to fluctuate throughout the sedimentation and thereafter. Among the detrital varieties, muscovite is more frequently observed (Plate 6.11). Detrital biotite, at most of the places have been chloritised due to oxidation (Plate 6.12). Abundance of authigenic biotite is found associated with carbonaceous fragments and coal seams. This is attributed to the anoxic conditions that generally prevails at swamps and depositories of coal and biotite is considered to crystallize under strong reducing conditions and be stable at elevated temperatures (Dapples, 1985). However, at many places near the coal seam, a considerable amount of biotite is chloritised indicating a shift towards a more oxidizing state. This is because, in Pranhita-Godavari basin, the coal deposition took place possibly in shallow areas which were exposed to atmospheric conditions for prolonged period causing widespread aerobic decay (Sen, 1979; Sanyal and Subramaniam, 1979).

Barakar sandstones exhibit conspicuous features which reflect equilibrium state between two minerals. The equilibrium phase is represented by the micas, where one mica mineral does not change entirely into another but the two occur intergrown within a single grain framework. Such equilibrium phase between the micas has been interpreted by Dapples (1985) to be one of the significant aspects of phyllo-morphic stage of diagenesis in sandstone. Biotite-chlorite (Plate 6.13) and chlorite-muscovite (Plate 6.14) assemblages show equilibrium phase among themselves. The equilibrium assemblage of muscovite-chlorite is stable in mildly oxidizing condition while that of chlorite-biotite in reducing condition. On slight change in Eh conditions, the equilibrium phase is disturbed and is displaced in favour of oxidized or reduced ions, thus favouring complete alteration and replacement.

At few places, the kaolinite matrix is replaced by calcite cement (Plate 6.15) replacement is partial to complete. Precipitation of calcite as cement in

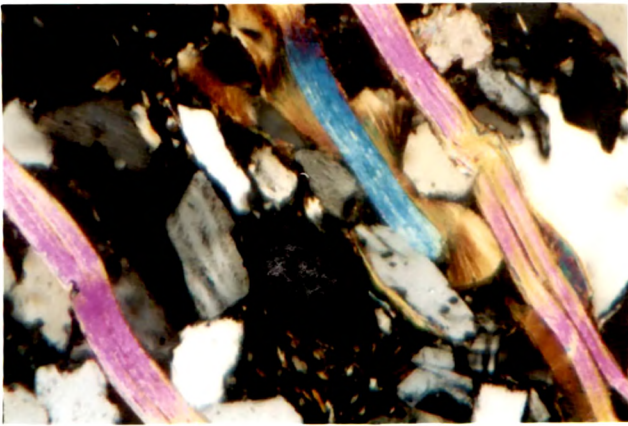
**Plate 6.11-6.15 Photomicrographs of Barakar Sandstones.**

**Plate 6.11** Detrital muscovites. (75X; Crossed Nicol).

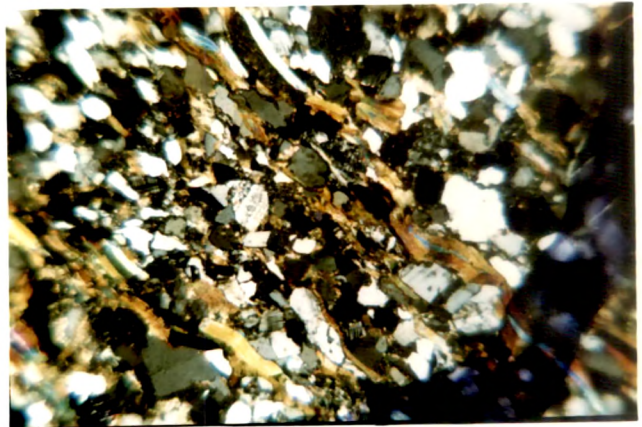
**Plate 6.12** Chloritisation of biotite. (40X; Crossed Nicol).

**Plates 6.13 & 6.14** Biotite-chlorite (6.13) and chlorite-muscovite (6.14), equilibrium assemblages indicating phylomorphic stage of diagenesis. (75X; Crossed Nicol)

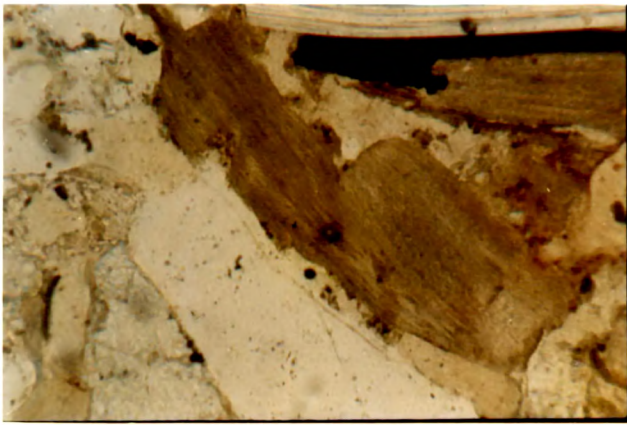
**Plate 6.15** Second-stage isomorphous replacement of kaolinite matrix by calcite (75X; Crossed Nicol).



6.11



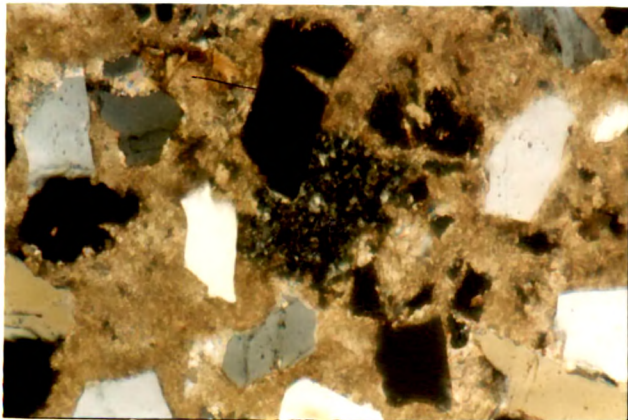
6.12



6.13



6.14



6.15

Barakar sandstone is rare, indicating the prevalence of acidic nature of pore solution within Barakar sandstone, also having kaolinite, which is stable in an acidic environment, as its principal matrix forming mineral.

### **BARREN MEASURES FORMATION**

Barren Measures Formation comprises predominantly of sandstones with subordinate variegated clays and micaceous siltstones.

In hand specimen, sandstones which constitute 85.1 % by volume of the formation, is medium to coarse grained, greenish-grey to greyish-white in colour. Predominance of greenish tinge is the main megascopic character to distinguish the Barren Measures sandstones from the underlying Barakar and overlying Lower Kamthi sandstones.

Under microscope Barren Measures sandstones exhibit fragmental texture comprising of 80 % framework particles and 20 % matrix. Grains are angular to sub-rounded and show moderate to poor sorting. Sandstones of Barren Measures are thus texturally immature. At places textural inversion (type 'd' of Lindholm, 1987) can be observed where well sorted unimodal grains are surrounded by matrix accounting for more than 5 % of the rock (Plate 6.16). Floating and point contacts are predominant. At places, plane and tangential contacts are also observed. Barren Measures sandstones show poor to moderate compaction.

Quartz is the dominant framework particle and it constitutes 60.19 % by volume of the sandstones (Table 6.2). Of the total quartz, 96.51 % are monocrystalline variety. Within the monocrystalline quartz, 95.09 % shows non-undulose extinction while the rest belongs to undulose variety. Feldspar accounts for 13.52 % by volume of the sandstone. Among the feldspars, microcline, orthoclase, perthites and plagioclase are observed in decreasing order of abundance. Next dominant framework particles are micas. Both detrital and authigenic varieties are encountered and are represented by biotite, muscovite and chlorite. (Chlorite although not a true mica, is nevertheless included within the micas because in most of the cases it was derived by chloritization of detrital biotite). Unstable rock fragments constitute

**Plate 6.16-6.20 Photomicrographs of Barren Measures Sandstones**

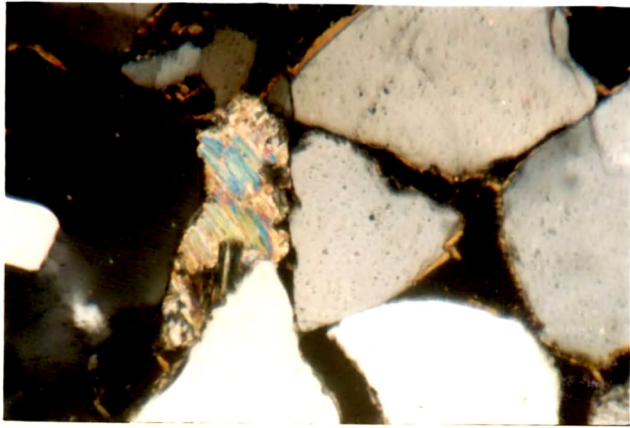
**Plate 6.16** Textural inversion. (75X; Crossed Nicol)

**Plate 6.17** Grain of garnet with inclusion of rutile needles  
(75X; PPL).

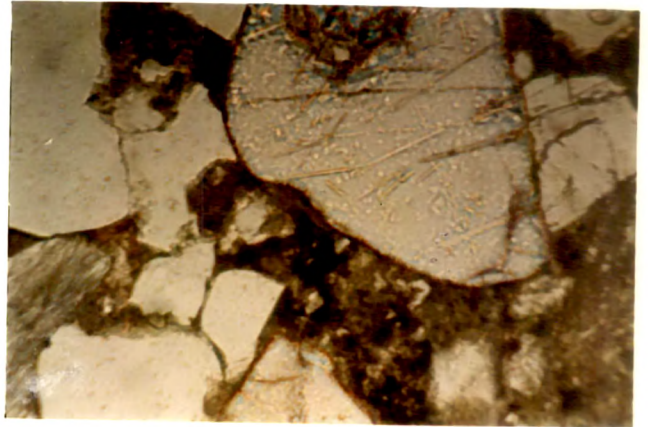
**Plate 6.18** Detrital argillaceous matrix. (100X; Crossed Nicol)

**Plate 6.19** Chloritic phyllosilicate cement showing clear  
transparency indicating absence of detritus.  
(75X; Crossed Nicol)

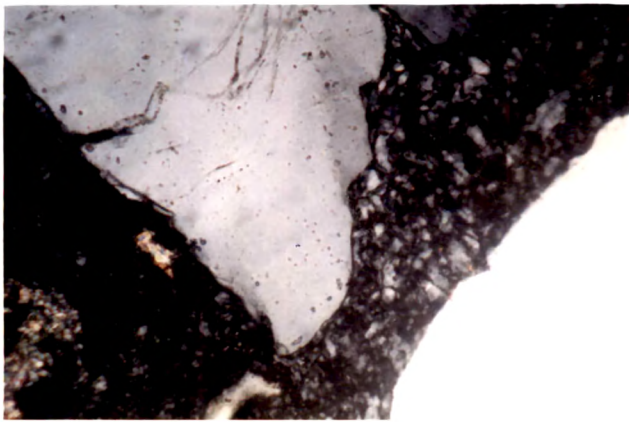
**Plate 6.20** Chloritic orthomatrix showing relict clastic texture  
with poor sorting of framework particles.  
(75X; Crossed Nicol)



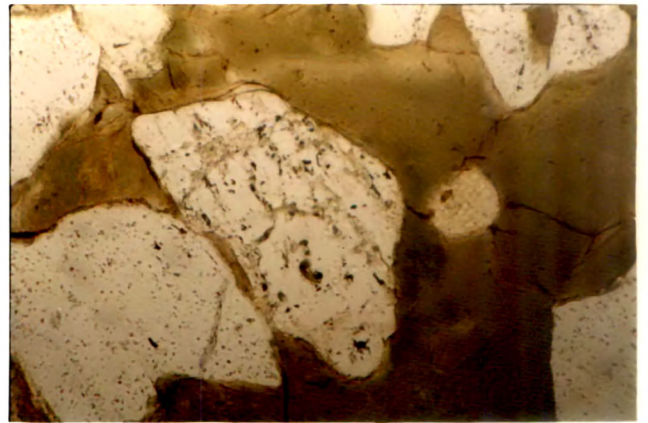
6.16



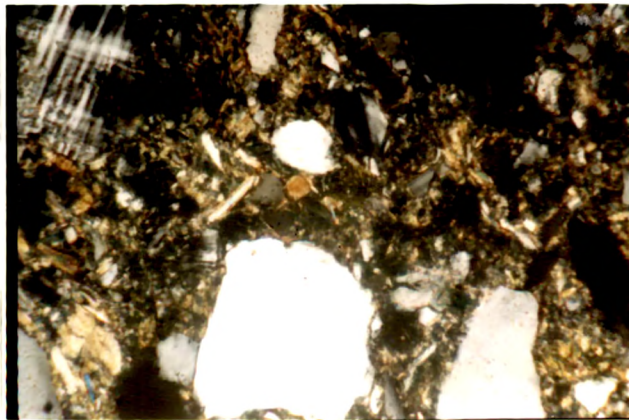
6.17



6.18



6.19



6.20

TABLE 6.2 : MODAL COMPOSITION OF BARREN MEASURES SANDSTONES

Sample No.	Depth (m)	Q U A R T Z						Rock Fragments	Mica	Accessories	Matrix	Cement	G/Rx
		Monocrystalline		Polycrystalline	Total	Feldspar	Total						
		Non Undulose	Undulose										
81/31	97.20	57.25	2.18	59.43	1.97	61.40	0.44	10.71	-	15	-	83:17:3	
81/32	106.00	59.38	3.78	63.16	-	63.16	0.29	7.86	1.45	-	15	83:16:1	
81/33	117.84	62.54	3.64	66.18	0.66	66.84	-	7.94	-	10	-	81:18:1	
81/36	124.75	56.12	-	56.12	2.79	58.91	-	5.57	0.80	20	-	76:20:4	
81/39	151.50	58.54	1.48	60.02	0.74	60.76	0.74	5.19	-	17	-	77:21:2	
81/44	180.00	56.40	2.23	58.63	3.19	61.82	2.23	0.32	0.32	35	-	91:11:8	
81/46	182.65	47.62	1.61	49.23	1.29	50.52	0.32	0.32	-	35	-	76:21:3	
81/53	270.00	66.85	1.88	68.73	1.13	69.86	0.75	1.18	1.69	13	-	82:16:2	
81/54	276.93	47.54	1.74	49.28	4.64	53.92	-	3.47	-	20	-	64:29:6	
81/56	288.50	55.96	2.90	58.86	2.32	61.18	0.29	4.06	-	22	-	80:17:3	
81/57	292.80	44.24	5.31	49.55	5.31	54.86	1.76	0.44	-	27	-	68:22:10	
81/58	299.44	47.48	1.08	48.56	2.70	51.26	1.52	0.54	-	30	25	65:29:6	
81/67	374.00	52.50	1.46	53.96	0.87	54.83	0.29	0.89	2.33	-	17	80:18:2	
81/71	406.25	63.14	2.37	65.51	5.92	71.43	-	2.35	0.89	-	-	81:12:7	
81/72	406.70	56.16	3.08	59.24	0.54	59.78	-	2.35	0.72	25	-	82:17:1	
81/73	413.68	61.55	3.22	64.77	0.21	64.98	0.43	2.79	2.57	14	-	80:19:1	
82/4	52.00	52.88	0.71	53.59	0.53	54.09	0.43	6.79	1.07	20	8	83:16:1	
82/6	68.50	64.14	2.01	66.15	0.67	66.82	-	12.42	-	10	-	85:14:1	
82/9	85.00	64.44	2.30	66.74	2.30	69.04	0.92	0.92	-	10	3	77:19:4	
82/11	97.50	42.85	1.14	43.99	2.85	46.84	0.28	3.42	6.00	30	-	73:22:5	
82/12	103.50	54.13	1.30	55.43	0.87	56.30	0.43	15.65	0.65	20	-	87:11:2	
82/13	109.00	48.53	0.44	48.97	3.54	52.51	0.59	6.64	4.27	23	-	74:20:6	
82/14	112.50	41.99	1.61	43.60	8.26	51.86	-	5.57	-	33	-	71:16:13	
82/20	153.50	60.05	4.21	64.26	2.49	66.75	0.35	13.01	0.53	15	-	85:16:3	
82/21	154.50	48.45	-	48.45	2.95	51.40	0.84	9.69	-	25	-	81:13:6	
82/25	160.50	46.05	0.73	46.78	1.15	47.93	0.73	7.32	0.10	-	35	81:16:3	
82/26	163.50	61.37	1.22	62.59	2.75	65.34	-	2.14	1.22	20	-	82:15:3	
82/27	164.50	62.31	3.39	65.70	2.54	68.24	0.42	0.84	-	17	5	85:14	
82/28	165.50	55.25	4.17	59.42	1.04	60.46	-	14.24	4.17	10	-	83:15:2	
82/29	174.00	47.85	1.56	49.41	3.32	52.73	-	1.76	8.75	25	-	77:18:5	
82/31	184.50	62.48	1.91	64.39	0.95	65.34	-	10.51	-	10	-	81:18:1	
82/34	212.50	60.07	0.64	60.71	2.14	62.85	-	13.89	-	8	5	83:14:3	
M1/7	107.50	61.92	3.26	65.18	-	65.18	0.65	3.91	9.12	12	-	88:11:1	
M1/9	121.00	53.86	2.37	56.23	-	56.23	0.95	2.37	2.61	16	-	71:28:1	

Contd

Sample No.	Depth (m)	Q U A R T Z						Rock Fragments	Mica	Accessories	Matrix	Cement	G:R
		Monocrystalline		Polycrystalline	Total	Feldspar							
		Non Undulose	Undulose										
M1/10	122.00	56.46	1.72	58.18	3.43	61.61	0.58	2.88	1.15	13	-	70:25:5	
M1/11	126.00	57.76	1.96	59.72	0.43	60.15	0.87	3.70	-	20	-	78:20:2	
M1/17	182.34	43.94	3.33	47.27	6.06	53.33	1.51	-	-	-	30	67:22:11	
M1/24	218.00	54.81	1.97	56.78	-	56.78	1.97	1.48	14.81	20	-	89:8:3	
M1/30	243.50	45.13	7.96	53.09	-	53.09	1.32	1.32	-	10	15	72:26:2	
M1/32	265.30	62.26	4.76	67.02	0.63	67.65	1.27	1.27	-	12	-	77:21:2	
M1/36	284.00	57.93	3.78	61.71	-	61.71	1.26	3.78	1.68	11	-	74:25:1	
M1/40	309.00	56.28	8.74	67.02	-	67.02	1.16	6.99	-	7	5	83:16:1	
M1/42	321.50	56.32	10.48	66.80	5.89	72.69	1.96	2.62	-	7	-	74:17:9	
M1/45	359.50	37.22	10.29	47.51	6.34	53.85	1.58	-	-	20	-	59:31:10	
M1/46	369.00	51.80	1.58	53.38	-	53.38	0.52	5.01	5.27	25	-	82:17:1	
M1/48	380.50	62.59	3.17	65.76	0.21	65.97	0.63	2.11	1.48	15	-	81:18:1	
M1/52	419.00	38.11	3.18	41.29	0.70	41.99	0.35	1.41	-	40	-	70:28:2	
C1/12	83.00	60.41	1.42	61.83	1.07	62.90	0.71	4.97	-	14	-	76:22:2	
C1/15	100.00	55.17	1.52	56.69	2.02	58.71	-	2.02	-	18	-	71:26:3	
C1/20	109.50	56.45	0.79	57.24	4.74	61.98	1.18	-	-	-	25	76:16:8	
C1/25	127.50	66.41	5.48	71.89	3.05	74.94	1.22	2.43	-	8	-	80:15:5	
C1/30	152.00	69.92	4.11	74.03	2.06	76.09	0.68	1.37	-	15	-	89:8:3	

a meagre 0.62 % of the rock while accessories (mostly garnets) make up 1.38 % by volume (Plate 6.17) of the Barren Measures sandstones.

Matrix of the Barren Measures sandstones is dominantly chlorite in composition. Where chlorite is absent, kaolinite takes its place. At places pure detrital argillaceous matrix is also seen (Plate 6.18). Cement, formed by replacement of the argillaceous and clayey matrix is calcareous in nature. Cement precipitation shows erratic relationship with depth and is not ubiquitous, although in some samples calcite cements constitute 35 % by volume of the rock.

Percentage of framework particles (Q→60.19, F→13.52, Rx→0.62, Mica and others →5.70 %) and matrix (20 %) points to the Barren Measures sandstones as falling in Dott's sub-arkosic (or arkosic) wacke category of sandstones.

## **DIAGENESIS**

Diagenesis in Barren Measures sandstones is characterized by alteration in both matrix as well as framework mineral composition.

Conspicuous greenish-grey colour of the Barren Measures sandstones is due to the dominance of chlorite which occurs both as a pore filling matrix and authigenically formed grains. The chlorite matrix is also authigenically formed from recrystallisation of trapped detrital clay. Pore-filling chlorite in Barren Measures sandstone is so diverse in its characteristic features that it can be classified into different categories as per Dickinson's (1970) classification.

- ◆ Phyllosilicate cement - Clear transparency indicating absence of minute detritus or impurities, monomineralogy indicating restricted composition and concentric colour zonation are some of the textural features of phyllosilicate (chloritic) cement (Dickinson, 1970) (Plate 6.19).
- ◆ Orthomatrix - Chlorite matrix recrystallized from detrital clay and showing relict clastic texture with poor sorting of framework particles is the feature of what is called orthomatrix by Dickinson (Op. cited) (Plate 6.20).

- ◆ **Epimatrix** - In some cases, Barren measures sandstones show well-sorted framework grains in a chloritic matrix lacking relict clastic texture but showing murky impurities. Some detrital grains are diagenetically altered. According to Dickinson (1970), such matrix may be termed as epimatrix (Plate 6.21).

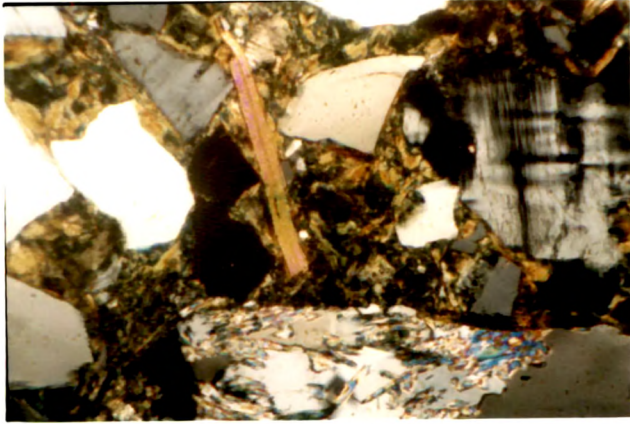
Dominance of chlorite matrix in Barren Measures sandstones may be attributed to a change in groundwater chemistry back to higher Iron and Magnesium ion concentrations as in Talchir times, indicating a return of aridity. Occurrence of intermittent kaolinite matrix is attributed to degradation of ferrigenous chlorite matrix due to high degree of leaching of the alkalies aided by high permeability conditions under which kaolinite is known to be stable (Degens, 1965). Variation in concentration of chlorite and intermittent appearance of kaolinite thus indicate fluctuations in the intensity of aridity during the Barren Measures time. Occurrence of well-crystallized chlorite flakes, occurring as patches or aggregates within the matrix is one of the important characteristic petrographic features of this sandstone (Plate 6.22). They were formed by aggradation of ferrigenous chlorite matrix by fixation of iron derived from dissolution of detrital biotite by the circulating pore solution. The process is associated with leaching of potassium from detrital biotite (Morad, 1982). Abundant flakes of chlorite crystals are observed in association with chloritised biotite in zones where calcite has replaced the clay matrix as a cement. This suggests that in a calcite precipitating environment, biotite tends to alter into chlorite which is more stable in that environment (Dapples, 1985) (Plate 6.23).

Authigenic biotite is lesser in Barren Measures sandstones as compared to Barakar sandstones. It appears mostly within the chlorite mass as an equilibrium mixture. Authigenic muscovite is seen in association with chlorite (Plate 6.24) and also independently. As discussed earlier in Barakar sandstone, chlorite-muscovite association is indicative of a slightly more oxidizing phyllo-morphic stage than that of biotite-chlorite association.

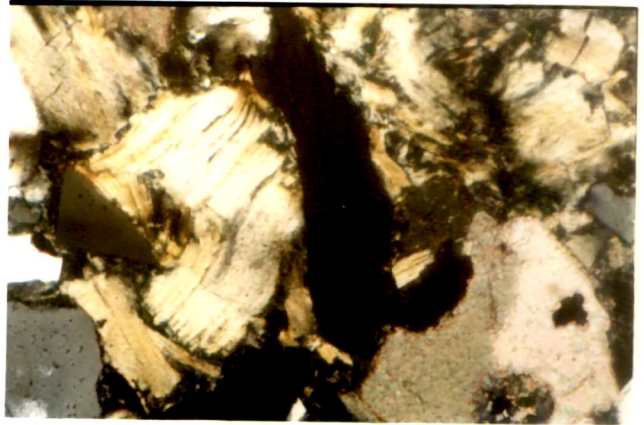
Examination of thin sections of Barren Measures sandstone reveals that upper part of the formation is characterized by more homogeneity and transparency in matrix composition (be it chloritic or kaolinitic). With depth

**Plate 6.21-6.25 Photomicrographs of Barren Measures Sandstones**

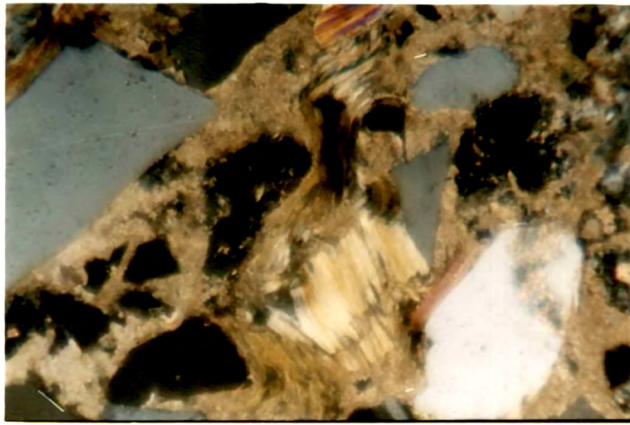
- Plate 6.21** Epimatrix showing murky impurities of detrital clay. Note the equilibrium assemblage of polycrystalline quartz and muscovite (bottom portion of the plate). (75X; Crossed Nicol)
- Plate 6.22** Well crystallised authigenic chlorite flakes. (75X; Crossed Nicol)
- Plate 6.23** Authigenic chlorite flakes formed due to alteration of biotite in a calcite precipitating environment. (75X; Crossed Nicol)
- Plate 6.24** Association of authigenic muscovite and chlorite. (40X; Crossed Nicol)
- Plate 6.25** Replacement of clay matrix by calcite. (100X; Crossed Nicol)



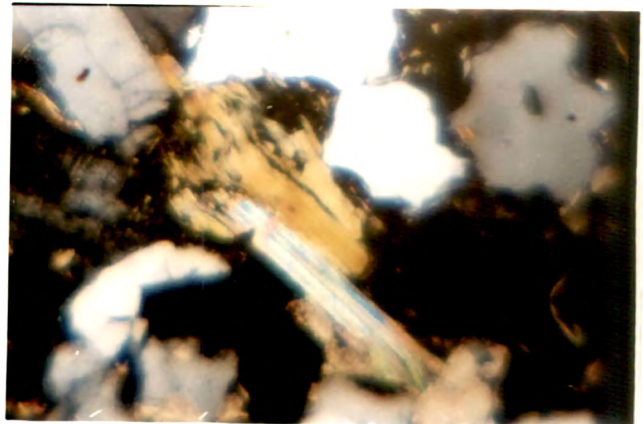
6.21



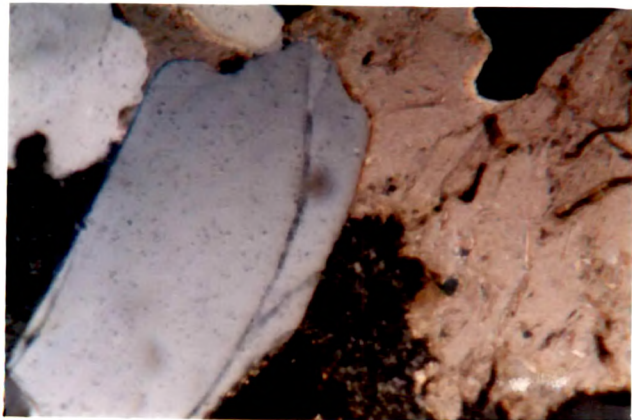
6.22



6.23



6.24



6.25

there is a distinct preference for segregation of micas in local clusters of crystal aggregates indicating an increase in the intensity of phylломorphism with depth (Dapples, 1970) within the Barren Measures sandstones.

Replacement of clay matrix by calcite is frequently observed in Barren Measure sandstone (Plate 6.25). At places the replacement is so complete that the sample does not contain any fraction of clay. In most of the cases silty and kaolinite clay matrix was replaced by calcite. Chlorite matrix, which is known to be stable in a calcite precipitating environment (Dapples, 1985) was by and large, unaffected by such replacement. Some samples show features like what has been termed by Foik (1965) as displacive precipitation. Here the calcareous cement was considerably sparsified resulting in the expansion of depositional framework (Plate 6.26). At places, the crystallization of calcite cement went to such an extent so as to result in the development of drusy and fibrous calcite crystals showing a preferred orientation of longest axis normal to the surface of detrital grains (Plate 6.27). Such development of calcite crystals may be attributed to a continuous circulation of pore water supersaturated with  $\text{Ca}^{++}$  and  $\text{CO}_3^{--}$  ions.

Among detrital grains, feldspars underwent maximum alteration and replacement. Orthoclase and microcline show partial replacement by secondary calcite (Plate 6.28). Solution rich in  $\text{Ca}^{2+}$  and  $\text{CO}_3^{2-}$  ions are capable of destroying the potash feldspar lattice by causing silica tetrahedral units to go into solution under a high pH which characterize the calcite precipitating solution. Replacement of plagioclase by calcite has also been noticed in few samples.

Barren Measures sandstones thus exhibit both locomorphic and phylломorphic stages of diagenesis. The fact that locomorphic stages can occur after the phylломorphic stage is typically exemplified by sections of some of the sandstone samples of Barren Measures, where replacement of clay matrix by calcite occurred later than the start of phylломorphic stage typified by crystallization of micas, as is evidenced by the textural interrelationship (Plate 6.29).

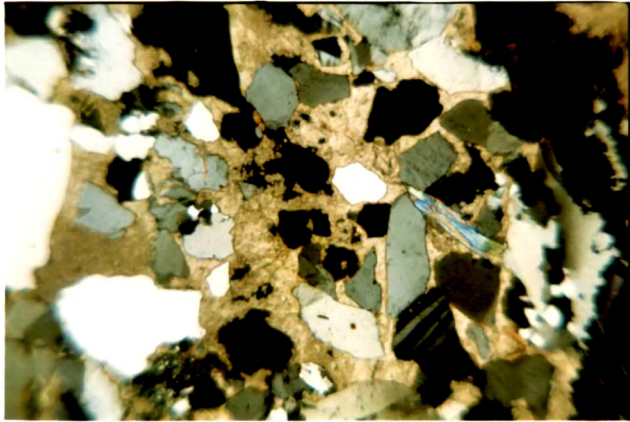
**Plate 6.26-6.29 Photomicrographs of Barren Measures Sandstones**

**Plate 6.26** Calcite cement showing displacive precipitation, resulting in expansion of depositional framework. (40X; Crossed Nicol)

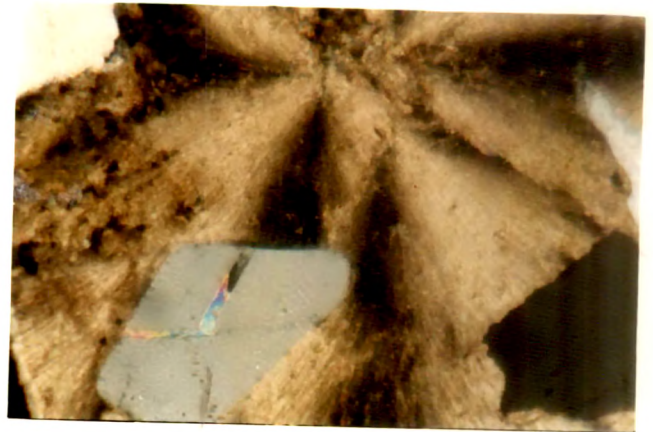
**Plate 6.27** Development of drusy fibrous calcite crystals as cement. (75X; Crossed Nicol).

**Plate 6.28** Replacement of microcline by calcite. (75X; Crossed Nicol)

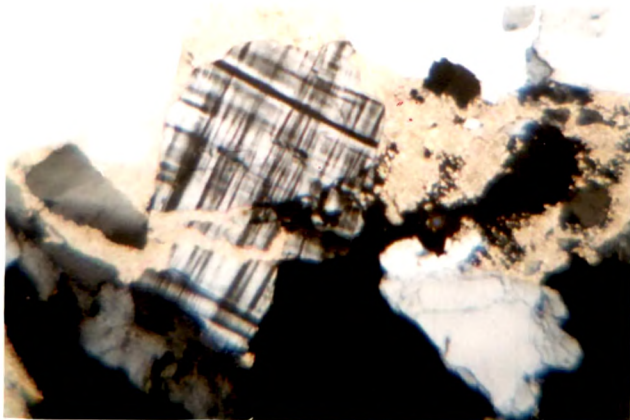
**Plate 6.29** Equilibrium assemblage of muscovite biotite and chlorite in a calcite precipitating environment. (75X; Crossed Nicol)



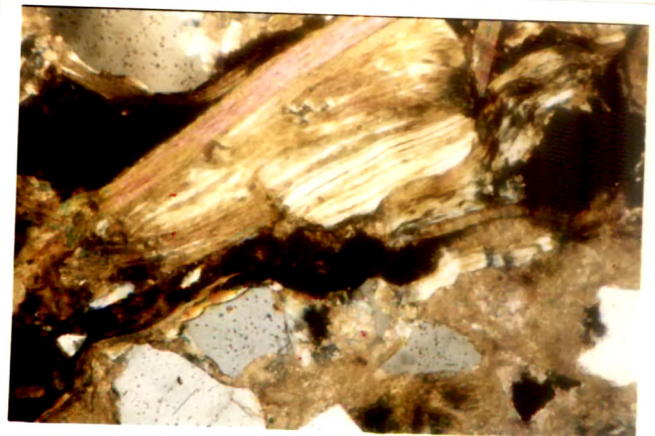
6.26



6.27



6.28



6.29

## KAMTHI FORMATION

Kamthi Formation can be divided lithologically into 3 units-Lower, Middle and Upper members. Lithology of these members have already been discussed in detail in earlier chapters.

Megascopically, the sandstones of the 3 members can be differentiated mainly on the basis of colour. Sandstones of the Lower Member are medium to coarse grained, greyish white and calcareous. Sandstone of the Middle Member is medium grained and greenish grey while the Upper Member sandstone is coarse grained ferruginous and red in colour.

Detail thin section studies of the Kamthi Formation are mainly confined to the Lower and Middle members because of their position in the Lower Gondwana Group. Few representative samples of the basal part Upper Kamthi member were studied under the microscope to examine the nature of change of the mineralogy from the Middle to the Upper Member.

Texturally, the rocks of Lower Kamthi Formation shows similarity to that of Barakar Formation. The sandstones show fragmental texture. The framework grains are medium to coarse grained, subrounded to sub-angular and moderately sorted. Compaction is poor.

Quartz forms 61.11 % by volume of the sandstones (Table 6.3). Of these, 97% percent are monocrystalline and 3 % are polycrystalline quartz. Of the monocrystalline quartz, 93 % are non-undulose variety while a sizeable 7% shows undulose extinction. Feldspar accounts for 12.83 % of the Lower Kamthi sandstones. Amount of unstable rock fragments, mica and accessories are 0.84 %, 3.28 % and 0.58 % respectively.

Average matrix content in Lower Kamthi sandstone is 15 %. Matrix is mainly argillaceous and kaolinitic and at places chloritic. Cement is generally calcareous in nature.

Thin section studies of Middle Kamthi Member was carried out on surface samples since cored samples were not available. Since the surface exposures

TABLE 6.3 : MODAL COMPOSITION OF KAMTHI SANDSTONES

Sample No.	Depth (m)	Q U A R T Z							Feldspar	Rock Fragments	Mica	Accessories	Matrix	Cement	Q:F:R:X
		Monocrystalline			Polycrystalline	Total									
		Non Undulose	Undulose	Total											
B1/2	2.25	56.68	6.80	63.48	0.57	64.05	17.01	1.70	6.23	-	11	-	77:20:3		
B1/10	60.70	68.21	3.32	71.53	-	71.53	8.45	0.30	1.81	0.90	17	-	89:10:1		
B1/11	65.51	38.01	11.03	49.04	9.81	58.85	3.68	2.45	-	-	20	15	75:6:19		
B1/12	65.61	57.64	5.64	63.28	0.81	64.09	11.28	0.40	3.22	-	16	5	83:15:2		
B1/17	71.66	56.08	4.49	60.57	1.49	62.06	14.95	0.37	3.36	2.24	14	3	78:19:3		
B1/18	72.70	54.08	4.91	58.99	0.98	59.97	19.17	-	7.37	1.47	12	-	75:24:1		
B1/19	74.93	48.94	2.02	50.96	2.22	53.18	15.97	1.62	1.21	-	7	21	72:23:5		
B1/20	75.22	49.55	1.86	51.41	1.24	52.65	16.11	0.62	0.62	-	5	25	74:23:3		
B1/26	83.47	67.25	1.18	68.43	0.39	68.82	10.39	0.20	8.23	2.35	10	-	86:13:1		
B1/29	95.08	52.94	1.25	54.19	1.50	55.69	13.55	0.75	-	-	30	-	78:19:3		
C1/2	21.50	51.25	3.13	54.38	2.20	56.58	11.30	0.80	5.32	-	18	8	79:17:4		
C1/6	47.50	61.34	3.28	64.62	1.25	65.87	12.16	0.93	2.04	-	20	-	82:15:3		
BMK1	Surface	59.65	2.10	61.75	1.70	63.45	14.50	0.70	1.35	-	5	20	78:18:4		
BMK6	Surface	57.30	2.07	59.37	1.82	61.19	12.57	0.47	1.73	-	5	19	80:17:3		
M2	Surface	62.38	3.49	66.32	2.42	68.74	12.81	1.61	4.83	-	-	13	80:15:5		
MMK1	Surface	49.67	4.51	54.18	1.04	55.22	12.07	0.69	-	-	7.5	24.5	80:18:2		

are very weathered in nature representative samples from different horizons within the member were subjected to microscopic studies.

The lower and middle part of the middle member shows textural similarity with the lower member in that the grains are subrounded and shows moderate sorting. The upper part of the middle member shows very poor sorting with a distinct bimodality in the quartz grains (Plate 6.30).

Average quartz content of the Middle Kamthi sandstone is 62.15 % of this, monocrystalline quartz is 97 %. Undulose quartz is lesser than the lower member and its amount is 5 %. Feldspar content shows an increase in the middle member and it accounts for 13 % by volume of the sandstone. Unstable lithic fragments and mica contents are 0.87 % and 1.97 % respectively. Interstitial substances account for 22.99 % by volume of the sandstone. Of this 19.37 % is the precipitated calcite and iron oxide cement (Plate 6.31). The rest 3.62 % is occupied by detrital argillaceous and chlorite and kaolinitic matrix.

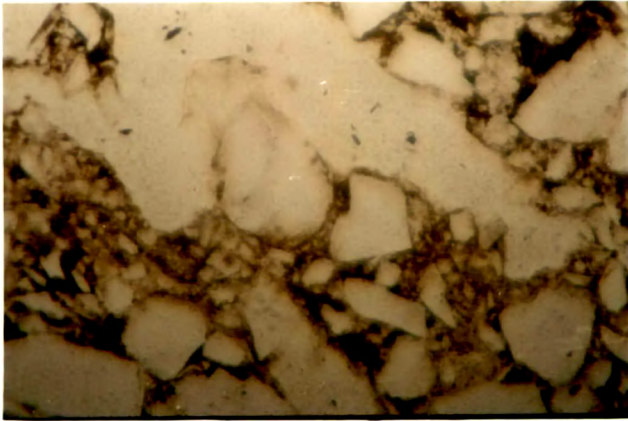
## **DIAGENESIS**

Diagenetic changes representing locomorphic stage dominated the Lower Kamthi sandstones. In the Lower part of the lower member kaolinite matrix is common. In the upper part the clay matrix is ubiquitously replaced by calcite (Plate 6.32). At places the replacement is total. Such ubiquitous development of carbonate may be attributed to abundance of dissolved CO<sub>2</sub> which may be provided in the upward-moving pore fluids generated by degradation of organic matter and kerogen in the Lower horizons (Sayyed and Patwardhan, 1992). Feldspar replacement by calcite is frequently encountered. Phyllo-morphic stage is not so pronounced as the Barakar or Barren Measures Formation. However in the lower part near the coal seam equilibrium assemblage of biotite and chlorite can be seen. Detrital biotite are much chloritised. Detrital muscovite is also encountered.

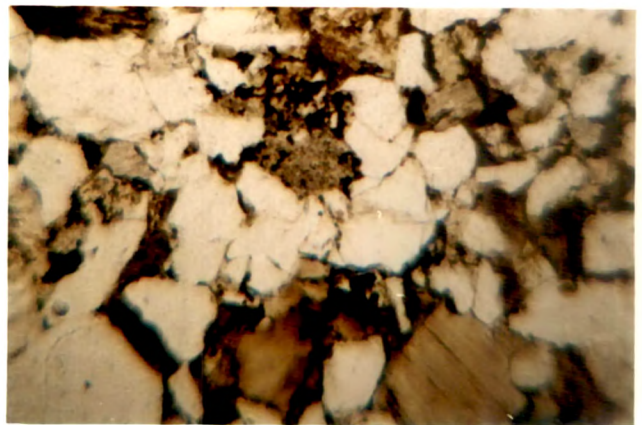
Sandstone of the middle Kamthi member is characterized by locomorphic as well as redoxomorphic stages. Phyllo-morphic stage is almost unrepresented. The near absence of phyllo-morphic stage may be due to the reason that the samples studied are surface samples and it is quite likely that micas formed during phyllo-morphism have been oxidized due to sub-aerial exposure.

**Plate 6.30-6.33 Photomicrographs of Kamthi Formation**

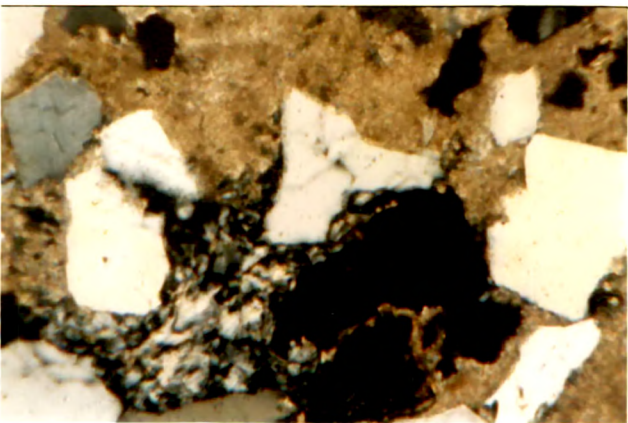
- Plate 6.30**      **Poor sorting and bimodality in the Middle Kamthi sandstone. (40X; PPL)**
- Plate 6.31**      **Late stage iron oxide cement in Middle Kamthi sandstone. (40X; PPL)**
- Plate 6.32**      **Clay matrix replacement by calcite in upper part of Lower Kamthi Member. (40X; Crossed Nicol)**
- Plate 6.33**      **Phyllosilicate chlorite cement showing distinct colour zonation in Middle Kamthi Sandstone. (75X; Crossed Nicol)**



6.30



6.31



6.32



6.33

The lower and middle part of the Middle member is characterized by a greenish tinge where in the upper part near the contact with upper Member the sandstones show a reddish tinge. These two colours are attributed to the presence of chlorite and hematite. The chlorite occurs as phyllosilicate cement (Dickinson 1976) (Plate 6.33) and as minute flakes within the detrital clay matrix. Hematite occurs as coating on the detrital particles and within the interstitial clay minerals (Plate 6.31). As discussed earlier, chlorite was formed from detrital biotite by leaching of  $K^+$  ions by circulating pore water in a mildly oxidizing environment. In a strongly oxidizing environment the diagenetic dissolution of detrital biotite resulted in almost complete release of iron into pore spaces forming fine hematite pigments, frequently corroding the detrital particles. According to Mc Bride (1974) slightly acidic condition of many streams tend to keep the iron primarily in the reduced form during transportation and red colour develops only after deposition in an environment of higher pH. Indeed, occurrence of hard concretations of calcareous material in the upper part of the middle member points to the fact that the existence of a very high pH environment during the closing stages of Middle Kamthi sedimentation was responsible for imparting a reddish tinge to the sandstone and a variegated appearance to the clay.

Petrographic examination of the basal part of Upper Kamthi Formation (purple sandstone) reveals that it is completely devoid of feldspar and cemented by ferruginous cement. The quartz grains are medium grained, rounded to sub-rounded and well sorted. At places the quartz grains show distinct bimodality where angular fine grains are seen occupying the interstitial portions between the bigger grains. Such textural characteristics and the conspicuous absence of feldspars suggest long transportation and deposition in a very warm humid climate.

## **DISCUSSIONS**

From the preceding paragraphs, it becomes amply clear that climate, intra-basinal tectonism and diagenesis left distinct imprints on the sandstones of Lower Gondwana Group.

During Gondwana sedimentation, the climatic conditions influencing production and deposition of sediments varied as a fluctuation of overall global

climatic changes and the movement of the Gondwana landmass from a position of 60°S latitude in early Permian to 38°S latitude by the end of Triassic (Crowel and Frakes 1970, Mc Elhinny, 1973 in Suttner and Dutta, 1986). This change in climatic conditions is manifested in the authigenic mineralogy and to a certain extent in the framework mineralogy of the sandstones of the study area.

As discussed earlier, presence of pore filling authigenic chlorite suggests an arid to semi-arid climate with a high concentration of iron and Magnesium ions in the groundwater. Occurrence of authigenic kaolinite, on the other hand, suggests a humid to wet climate, resulting in dilution of the pore water with respect to ferromagnesian ions. These two minerals mostly occur as pore-filling matrix (Although authigenic in origin these two minerals, when occurring as an interstitial pore filling, are not termed as cement but as matrix according to Dickinson's (1970) terminology to distinguish them from calcite and iron oxide cement which were paragenetically formed much after chlorite and kaolinite by replacement of the latter. Biotite and unstable lithic fragments were the chief contributors of  $Fe^{++}$  and  $Mg^{++}$  ions for the formation of chlorite and  $Fe^{3+}$  ions for the precipitation of iron-oxide cement. Although there is no petrographic evidence, presence of iron and magnesium ions in the pore solution, required for the formation of chlorite and hematite, might have come from other mafic silicate minerals like hornblende and pyroxenes. These minerals have presumably disappeared during the course of diagenetic alterations due to their high instability. Both chlorite and kaolinite matrices are the products of climate-controlled ground water chemistry and are formed by locomorphic replacement of detrital clay matrix. Because of their presence in varying proportions at different depths of different formations, it is concluded that depth-related diagenetic controls were not responsible for the precipitation of chlorite and kaolinite matrices.

Effect of burial diagenesis on the detrital framework mineralogy is also minimal. If all sediments were subjected to burial diagenesis, preferential destruction of feldspars and polycrystalline quartz would have taken place and that too, the extent of destruction would have increased systematically with depth. As evidenced from the modal composition of sandstones of different formations (Table 6.1, 6.2, 6.3), the variation in the percentages of feldspars and polycrystalline quartz varies haphazardly or in an irregular cyclic manner rather than in an unidirectional fashion.

From the overall Q : F : Rx ratio and compositional maturity of the Gondwana sandstones and the nature of early formed authigenic minerals (chlorite and kaolinite) it can be concluded that climate during the Lower Gondwana sedimentation changed from a cold, semi-arid (Talchir) to temperate humid (Barakar) to warm, semi-arid (Barren Measures) to warm-semi-humid (Lower and Middle Kamthi) to warm humid (Upper Kamthi). This inference is in concurrence with the mio-floral assemblage study of Srivastava and Jha (1987).

	Talchir	Barakar	Barren Measures	L. Kamthi	M. Kamthi
Q : F : Rx	88:5:7	89:15:1	81:18:1	82:17:1	82:17:1
Compositional (Q/F+Rx)	7.33	5.05	4.25	4.47	4.48

Compositional maturity, although controlled to a large extent by climate, also depends on the combined effects of relief and transport history. Talchir sedimentation took place much near to the young fault block Pakhal and Sullavai hill ranges. Abundant limestone fragments in Talchir sandstones justifies this view. Depletion of feldspars in Talchir sandstones may be attributed to a very high pH environment which resulted in its preferential replacement. Also fully kaolinised feldspars contain needles of muscovite which may be the initiation of formation of illite crystals.

With time, gradient of depositional slope reduced and the distance of transport increased. During Barakar sedimentation, of coarse, the relief was not low enough and the transport distance not high enough for the feldspars to be altered drastically. This is the reason, why in spite of prevalence of a humid climate, Barakar sandstones contain considerable amount of fresh feldspars. Rapid sedimentation and quick burial also helped in mitigating the effect of atmospheric weathering of some of the feldspars. On the other hand presence of some altered feldspars in Barren Measures sandstones, which, going by the warm semi-arid climate, should contain fresh feldspars, point to the more

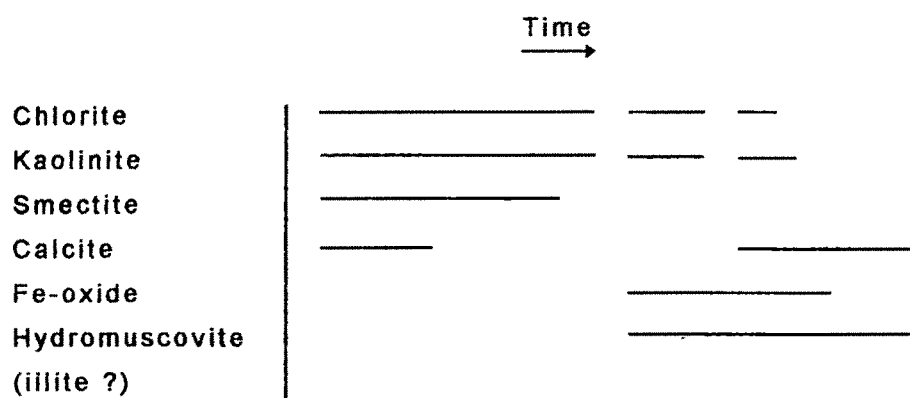
lowering of relief and increase in distance of transport. Similar is the case during Lower and Middle Kamthi whose lower feldspar content points to the return of humidity and a more greater transportation history. Supermature quartz-arenites of Upper Kamthi Formation indicate a very warm humid climate and very low relief.

At many places feldspars were altered diagenetically due to fluctuations in pH condition. Such alterations were specifically seen in a sandstone where calcite has precipitated as a late cement. Feldspars are unstable in an environment of high pH. But the formation of calcite cement is at certain horizons and not all-pervading through out the sequences. Detrital mineralogy of the Gondwana sandstones of the study area thus exhibits the presence of influence of both climatic conditions and tectonic stability, although overall mineralogy points to a more pronounced effect of the former than the latter.

Although depth related diagenetic changes had little influence on the framework mineralogy and authigenic matrix, detrital micas show significant diagenetic changes which are characterised by some signatures of depth related processes. Presence of authigenic micas concentrated in clusters within the pre-existing matrices of Barren Measures sandstones suggests that the Barren Measures sandstones had already attained phyllo-morphic stages. This reached an advanced stage in the Barakar sandstones which is typified by equilibrium assemblages of biotite-chlorite and muscovite-chlorite. Not uncommonly muscovite, biotite and chlorite have been encountered in the same-thin section, but one is more predominant than the others. According to Dapples (1970) this can be interpreted as a preferential control on mica authigenesis by the pH and Eh of the fluids in the pores at the time of deposition. The Talchir sandstone conspicuously does not show any presence of detrital or authigenic mica flakes. The Talchir sandstone analyzed in the present study is from the upper part of the formation and from near the contact with Barakar Formation. These sandstones represent an outwash deposit formed by high discharge of glaciated melt water. It is quite likely that intense leaching in a relatively warm temperature dissolved the detrital micas thus liberating  $Fe^{++}$  and  $Mg^{++}$  ions for chloritisation of the detrital matrix.

The paragenetic sequence of mineral formation in Barakar sandstones is thus characterized by two stages. The first and early stage was typified by

formation of Kaolinite and chlorite clay matrix from the trapped detrital clay and this stage is mainly climate controlled. The second stage is dominated by replacement and alteration of detrital and authigenic grains and recrystallization of authigenic clay matrices into neoformed micas. Calcite and iron-oxide cement were precipitated during this stage. This stage was influenced by Eh-pH controlled and to some extent depth-controlled diagenetic processes. Generalized paragenetic sequence of authigenic minerals is proposed by the author from his study is as follows.



The first paragenetic stage is of locomorphic type where substitution of detrital clay matrix by chlorite, kaolinite or smectite took place. The second paragenetic sequence is dominated by all three stages of clastic diagenesis proposed by Dapples (1985) - redoxomorphic stage, locomorphic stage and phyllomorphic stage. These stages did not form distinct episodes or did not necessary by operate independently. Rather, quite frequently, changes represented by these stages have been found in the same section. And in many sections it has been found that the reactions of locomorphic stage took place after the phyllomorphic stage. As noted by Dapples (1985) several generations of locomorphism may be indicated in a rock. This is particularly true for the Lower Gondwana sandstones where the whole sequence is characterized by locomorphic changes represented by replacement of one particular mineral by another one.

### X - RAY DIFFRACTOGRAMS

Lower Gondwana sandstones are very often intercalated with fine clastics and their identification is not possible under normal petrological microscope.

Colour index and physical characters of these units have been discussed in chapter 4. However, some important and conspicuous shale and clay units from individual formation were selected for X-Ray diffraction with an aim to identify their major constituents which can supplement the microscopic studies.

The X-Ray diffraction studies on 12 samples selected from boreholes and surface exposures were carried out using the method suggested by Griffin (1971). The powder of individual sample was allowed to pass through # 325 A.S.T.M. mesh and was later subjected to X.R.D. analysis. The instrument used was Rigaku, D. Max III (capacity 3KVA; Cu Tube, 2.2 K). Samples were scanned from  $10^{\circ}$  to  $50^{\circ}$ . The computerised values of  $2\theta$ , d-spacings and intensities obtained from the graphs (Fig. 6.1 to 6.12) were compared with the standard charts of different minerals (Griffin, 1971; and J.C.P.D.S. cards, 1974). The minerals have been identified formation wise in terms of a)  $2\theta$  value b) d-spacing and c) intensities as per standard methods in the X-Ray diffraction studies. (Table 6.4 to 6.15). However the minor peaks and the shoulder peaks could not be identified on account of overlapping and mixing.

## **INTERPRETATION**

The most notable feature observed from the results of X-Ray diffraction is the dominance of quartz with 100 % intensity peak in shale and clay samples of all the formations. This is on account of derivation of the sediments from granitic and gneissic terrain (discussed in detail in the provenance chapter).

Muscovite is the second important mineral that is characterised by its ubiquitous occurrence in all the formations. This abundance of muscovite can be attributed to either source rock lithology or to authigenesis. Pegmatite rich acidic igneous rocks (granite) can contribute substantial amount of detrital mica. Alternatively, crystallization of authigenic muscovite and quartz can take place due to destruction of clay minerals unstable in burial environment (Dapples, 1972, p. 22). As seen in the thin section study (Plates 6.11 and 6.21) both types of muscovite are present in Lower Gondwana sandstones. Abundance of muscovite in the Lower Gondwana shales and clays and similarly be attributed both source rock lithology as well as burial diagenesis. Of the feldspars, K-feldspars in form of orthoclase and microcline is dominant in Barakar, Barren Measures and Kamthi shale/clay whereas in Talchir argillites it

**TABLE 6.4 : XRD RESULTS OF SAMPLE P3 (TALCHIR DIAMICTITE).**

No.	2-THETA	d-spacing	I/10	Minerals
1	18.810	4.714	8	Apatite
2	19.850	4.469	4	Muscovite
3	20.840	4.259	24	Quartz
4	23.070	3.852	10	Calcite
5	24.020	3.702	19	Heulandite ?
6	26.630	3.345	100	Quartz
7	29.430	3.033	91	Calcite
8	31.460	2.841	3	Calcite
9	35.510	2.526	5	Apatite ?
10	36.010	2.492	13	Calcite
11	36.540	2.457	7	Quartz
12	39.460	2.282	21	Quartz, Calcite
13	40.270	2.238	3	Quartz
14	42.440	2.128	6	Quartz
15	43.210	2.092	14	Calcite
16	45.020	2.012	3	Chlorite
17	45.770	1.981	3	Quartz
18	47.180	1.925	5	Calcite
19	47.560	1.910	12	Calcite ?
20	48.560	1.873	15	Calcite
21	48.660	1.870	10	Analcite
22	50.130	1.818	7	Quartz
23	54.880	1.672	4	Quartz, Chlorite
24	56.590	1.625	4	Calcite
25	57.460	1.603	8	Calcite
26	59.940	1.542	7	Quartz, Chlorite

**Fig. 6.1 : XRD Graph of sample P3.**

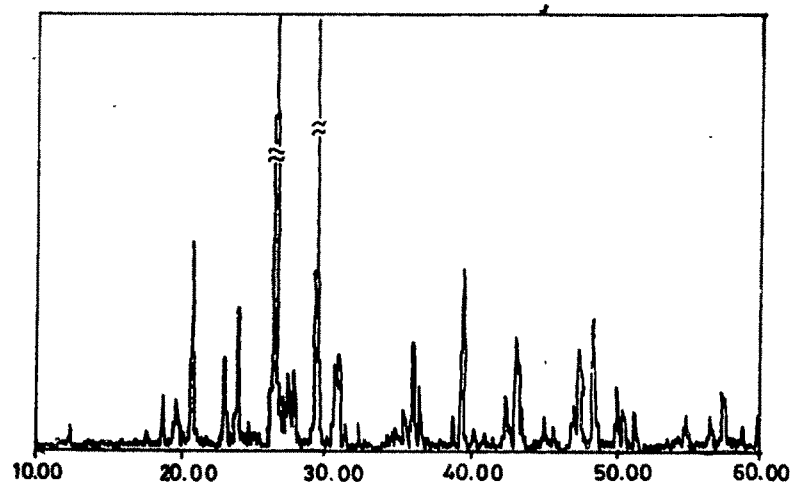


**TABLE 6.5 : XRD RESULTS OF SAMPLE P4 (TALCHIR CLAY).**

No	2-THETA	d-spacing	I/I0	Minerals
1	13 900	6 366	2	Plagioclase
2	20 880	4 251	23	Quartz
3	21 990	4 039	3	Plagioclase
4	23 110	3 846	4	Plagioclase
5	24 040	3 699	21	Plagioclase
6	24 320	3 657	3	Hematite, Plagioclase
7	25 110	3 544	3	Phillipsite
8	25 510	3 489	3	Muscovite, Plagioclase
9	26 660	3 341	100	Quartz
10	27 000	3 300	4	Plagioclase
11	27 780	3 209	7	Plagioclase
12	27 970	3 187	35	Phillipsite ?
13	29 460	3 030	29	Calcite ?
14	30 530	2 926	2	Plagioclase
15	31 320	2 854	3	Calcite
16	32 920	2 719	2	Phillipsite
17	34 930	2 567	3	Muscovite
18	35 090	2 555	3	Plagioclase
19	35 230	2 545	3	Plagioclase ?
20	35 540	2 524	4	Biotite
21	36 550	2 456	8	Quartz
22	39 480	2 281	12	Quartz, Biotite
23	40 310	2 236	4	Quartz
24	42 480	2 126	6	Quartz
25	43 620	2 073	2	Hematite
26	45 800	1 980	4	Quartz, Plagioclase
27	47 240	1 923	2	Plagioclase, Calcite
28	47 580	1 910	4	Biotite, Phillipsite
29	48 560	1 873	5	Calcite
30	50 150	1 818	14	Quartz
31	50 730	1 798	3	Gibbsite
32	54 890	1 671	4	Quartz, Biotite
33	57 450	1 603	3	Quartz
34	59 980	1 541	11	Quartz, Biotite
35	60.140	1.537	6	Biotite

**Fig. 6.2 : XRD Graph of sample P4.**

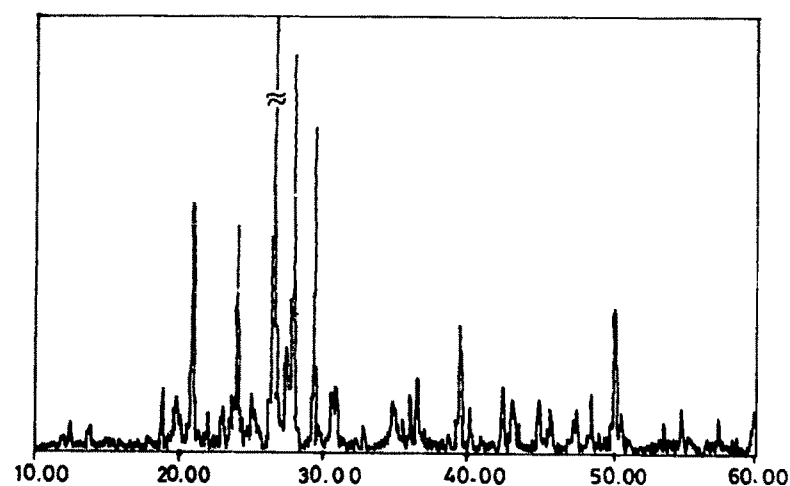


**TABLE 6.6 : XRD RESULTS OF SAMPLE P23 (TALCHIR NEEDLE SHALE).**

No.	2-THETA	d-spacing	I/10	Minerals
1	12.500	7.056	3	Kaolinite
2	19.830	4.474	5	Muscovite, Vermiculite
3	20.110	4.412	4	Muscovite
4	20.910	4.245	22	Quartz
5	22.070	4.024	4	Plagioclase
6	24.190	3.676	5	Plagioclase
7	25.340	3.512	3	Plagioclase
8	26.690	3.337	100	Quartz
9	27.560	3.234	23	Sphene
10	28.220	3.160	9	Biotite
11	28.410	3.139	3	Kaolinite
12	29.900	2.986	3	Muscovite, Sphene
13	35.060	2.557	5	Kaolinite, Muscovite, Plagioclase
14	35.670	2.515	4	Biotite
15	36.600	2.452	9	Quartz, Biotite
16	37.020	2.426	3	Plagioclase
17	39.530	2.278	9	Quartz, Plagioclase, Biotite
18	40.360	2.233	4	Quartz
19	42.510	2.125	10	Quartz, Kaolinite
20	43.300	2.088	5	Vermiculite Quartz
21	45.850	1.978	4	Muscovite, Kaolinite
22	50.170	1.817	11	Quartz
23	54.890	1.671	5	Quartz, Chlorite, Biotite
24	59.990	1.541	10	Quartz, Chlorite, Biotite

**Fig. 6.3 : XRD Graph of sample P23.**

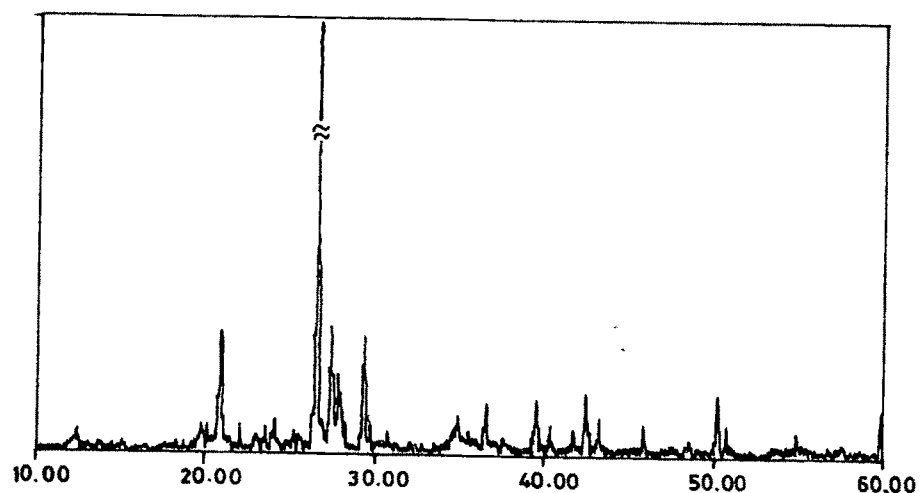


**TABLE 6.7 : XRD RESULTS OF SAMPLE P10 (TALCHIR CLAY).**

No	2-THETA	d-spacing	I/10	Minerals
1	20.860	4.255	21	Quartz
2	21.250	4.178	2	Kaolinite
3	24.920	3.570	15	Kaolinite
4	25.360	3.509	3	Plagioclase
5	25.600	3.477	2	Plagioclase
6	26.640	3.343	100	Quartz
7	34.550	2.594	2	Muscovite, Vermiculite
8	34.970	2.564	4	Plagioclase, (Kaolinite)
9	35.440	2.531	3	Kaolinite
10	36.030	2.491	3	Muscovite, Kaolinite
11	36.550	2.456	8	Quartz
12	37.780	2.379	3	Kaolinite
13	39.460	2.282	6	Quartz
14	42.450	2.128	7	Kaolinite
15	45.380	1.997	2	Glaucosite
16	45.570	1.989	2	Kaolinite
17	50.140	1.818	13	Glaucosite
18	54.880	1.672	5	Chlorite
19	55.050	1.667	4	Glaucosite, Phillipsite
20	55.290	1.660	4	Kaolinite
21	59.946	1.542	7	Chlorite, Kaolinite

**Fig. 6.4 : XRD Graph of sample P10.**

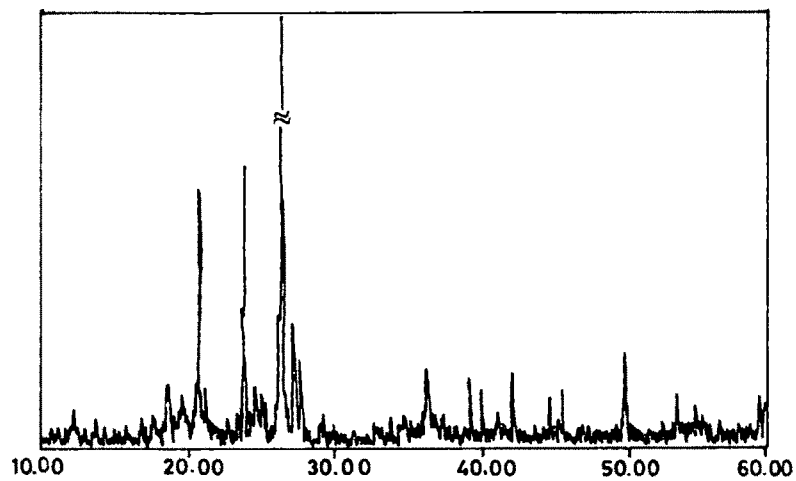


**TABLE 6.8 : XRD RESULTS OF SAMPLE P13 (BARAKAR CLAY).**

No	2-THETA	d-spacing	I/I0	Minerals
1	20.940	4.239	20	Orthoclase
2	21.470	4.135	3	Kaolinite
3	24.970	3.563	22	Orthoclase, Kaolinite
4	25.720	3.461	4	Orthoclase
5	26.700	3.336	100	Quartz, Orthoclase
6	29.820	2.994	7	Orthoclase ?
7	34.950	2.565	5	Kaolinite
8	35.130	2.552	5	Vermiculite
9	35.550	2.523	4	Kaolinite ?
10	36.040	2.490	5	Kaolinite
11	36.620	2.452	10	Quartz
12	37.550	2.393	2	Vermiculite
13	39.520	2.278	8	Quartz
14	40.330	2.235	3	Quartz
15	42.520	2.124	6	Quartz
16	45.640	1.986	3	Kaolinite
17	45.820	1.979	4	Quartz
18	48.100	1.890	2	Kaolinite
19	50.190	1.816	12	Quartz
20	50.620	1.802	3	Quartz
21	54.670	1.678	2	Vermiculite?
22	55.360	1.658	4	Quartz
23	56.850	1.618	2	Kaolinite
24	57.160	1.610	2	Quartz
25	59.980	1.541	81	Quartz

**Fig. 6.5 : XRD Graph of sample P13.**

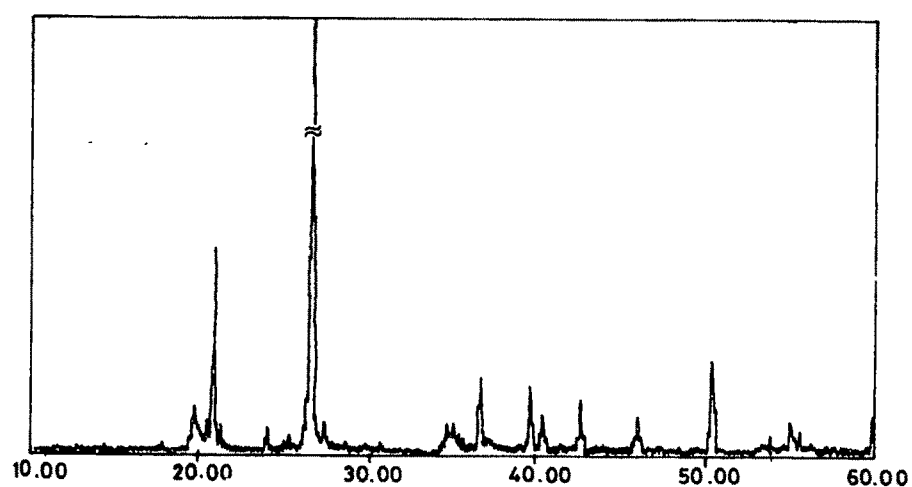


**TABLE 6.9 : XRD RESULTS OF SAMPLE M1/69 (BARAKAR SHALE).**

No.	2-THETA	d-spacing	I/10	Minerals
1	20.880	4.251	27	Quartz
2	24.900	3.573	9	Kaolinite, Microcline
3	26.650	3.342	100	Quartz
4	34.950	2.565	5	Kaolinite
5	36.540	2.457	9	Quartz
6	37.640	2.388	3	Orthoclase, Kaolinite
7	38.420	2.341	3	Kaolinite
8	39.480	2.281	5	Quartz
9	59.960	1.542	9	Kaolinite

**Fig. 6.6 : XRD Graph of sample M1/69.**

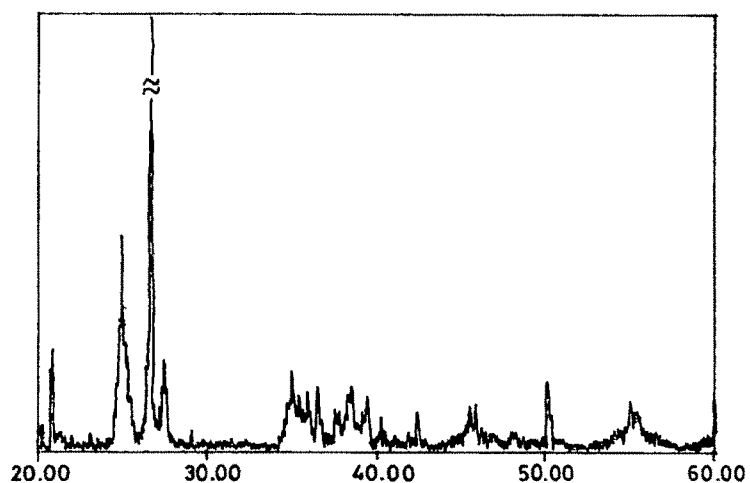


**TABLE 6.10 : XRD RESULTS OF SAMPLE P27 (BARAKAR CARBONACEOUS SHALE).**

No.	2-THETA	d-spacing	I/10	Minerals
1	20.900	4.247	22	Quartz
2	24.050	3.697	24	Heulandite, Dolomite ?
3	25.590	3.478	4	Corundum, Microcline
4	26.670	3.340	100	Quartz
5	27.470	3.244	11	Microcline
6	27.580	3.234	9	Diopside ?
7	36.590	2.454	7	Quartz
8	50.150	1.818	8	Quartz
9	59.970	1.541	7	Quartz

**Fig. 6.7 : XRD Graph of sample P27.**

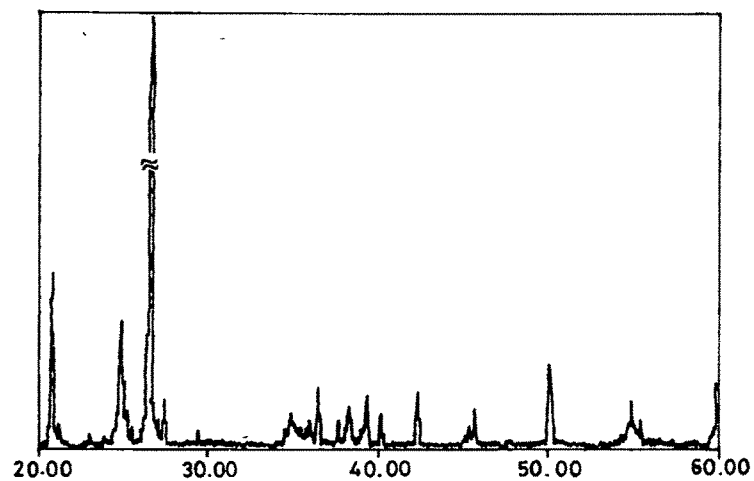


**TABLE 6.11 : XRD RESULTS OF SAMPLE P26 (BARAKAR CLAY).**

No.	2-THETA	d-spacing	I/I0	Minerals
1	19.750	4.492	4	Muscovite, Chloritoid ?
2	20.520	4.235	3	Muscovite ?
3	20.890	4.249	23	Quartz, Orthoclase?
4	24.100	3.690	2	Hematite
5	26.680	3.339	100	Quartz
6	27.510	3.240	3	Sphene, Microcline
7	34.610	2.590	2	Muscovite, Sphene, Glauconite
8	35.030	2.560	3	Muscovite, Siderite
9	35.390	2.534	2	Orthoclase
10	36.580	2.455	8	Quartz
11	39.590	2.279	7	Quartz
12	42.490	2.126	6	Quartz
13	45.830	1.978	4	Quartz
14	50.180	1.817	11	Quartz
15	54.900	1.671	4	Quartz
16	55.360	1.658	2	Quartz
17	59.990	1.541	8	Quartz

**Fig. 6.8 : XRD Graph of sample P26.**

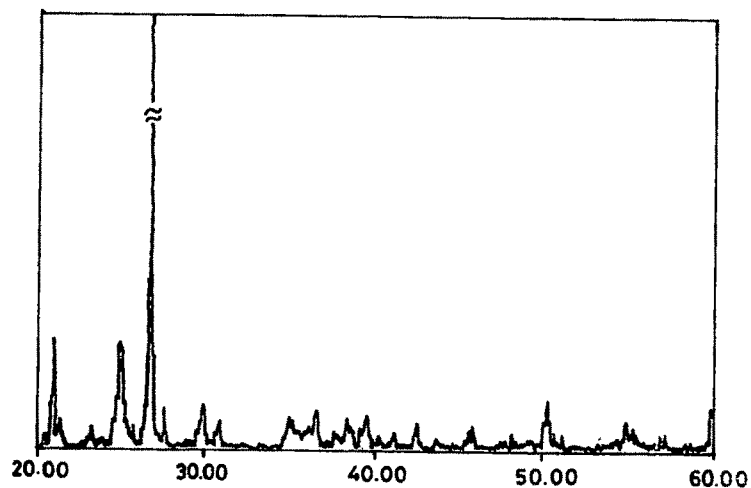


**TABLE 6.12 : XRD RESULTS OF SAMPLE C1/23 (BARREN MEASURES CLAY).**

No.	2-THETA	d-spacing	I/10	Minerals
1	20.850	4.257	18	Quartz
2	24.910	3.572	38	Kaolinite
3	25.060	3.551	23	Muscovite
4	25.280	3.520	15	Chamosite
5	25.610	3.476	6	Muscovite
6	26.650	3.342	100	Quartz
7	27.110	3.287	6	Microcline?
8	34.650	2.587	6	Muscovite
9	34.930	2.567	13	Muscovite, Kaolinite ?
10	35.440	2.531	8	Microcline
11	35.720	2.512	6	Chamosite, Kaolinite
12	35.980	2.494	10	Muscovite, Kaolinite
13	36.550	2.456	11	Quartz
14	37.580	2.391	5	Muscovite, Vermiculite
15	37.830	2.376	9	Kaolinite
16	38.930	2.342	5	Chamosite
17	39.190	2.297	6	Kaolinite
18	39.440	2.283	8	Quartz
19	39.560	2.276	7	Vermiculite
20	40.270	2.238	6	Quartz
21	42.460	2.127	6	Quartz
22	45.540	1.990	6	Muscovite, Kaolinite
23	45.790	1.980	8	Quartz
24	50.160	1.817	12	Quartz
25	54.930	1.670	7	Quartz
26	55.320	1.659	7	Quartz
27	55.600	1.652	5	Muscovite
28	59.970	1.541	10	Quartz

**Fig. 6.9 : XRD Graph of sample C1/23.**

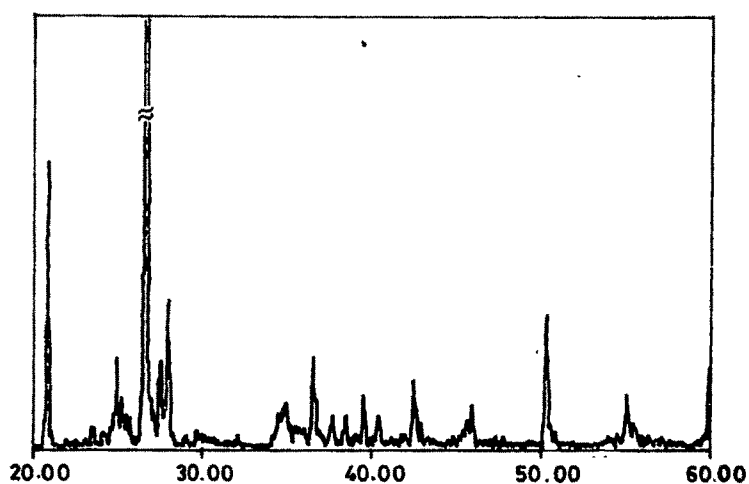


**TABLE 6.13 : XRD RESULTS OF SAMPLE M1/58 (BARREN MEASURES CLAY).**

No.	2-THETA	d-spacing	I/10	Minerals
1	20.870	4.253	19	Quartz
2	23.540	3.776	3	Muscovite,Orthoclase ?Albite (low)
3	25.330	3.513	6	Chamosite,Albite (low)
4	25.640	3.472	4	Muscovite
5	26.660	3.341	100	Quartz
6	27.170	3.279	4	Chamosite
7	27.490	3.242	9	Microcline
8	27.960	3.189	10	Muscovite ? Albite ?
9	34.710	2.582	4	Pyrope
10	35.100	2.555	4	Microcline,Chlorite ?
11	35.580	2.521	4	Chamosite
12	35.810	2.506	4	Hematite
13	36.570	2.455	9	Quartz, Garnet ?
14	37.800	2.378	4	Muscovite
15	38.440	2.340	4	Garnet ?
16	39.520	2.278	4	Quartz, Hematite ?

**Fig. 6.10 : XRD Graph of sample M1/58.**

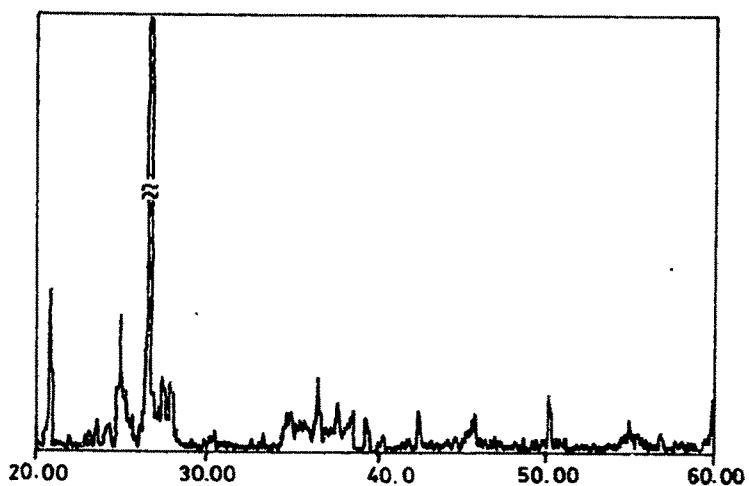


**TABLE 6.14 : XRD RESULTS OF SAMPLE C1/41 (BARREN MEASURES SHALE).**

No.	2-THETA	d-spacing	I/10	Minerals
1	20.850	4.257	24	Quartz
2	24.910	3.572	7	Microcline
3	26.630	3.345	100	Quartz
4	27.070	3.291	4	Microcline
5	27.500	3.241	26	Microcline
6	27.920	3.193	10	Albite
7	34.720	2.582	4	Garnet, Sanidine
8	34.950	2.565	6	Albite, Diopside
9	35.470	2.529	4	Diopside
10	35.820	2.505	4	Apatite
11	36.510	2.459	8	Quartz, Garnet
12	39.450	2.282	6	Quartz
13	40.270	2.238	4	Quartz
14	42.450	2.128	7	Quartz
15	49.890	1.976	3	Quartz
16	50.110	1.819	13	Quartz
17	54.890	1.671	4	Quartz
18	59.940	1.542	9	Quartz

**Fig. 6.11 : XRD Graph of sample C1/41.**

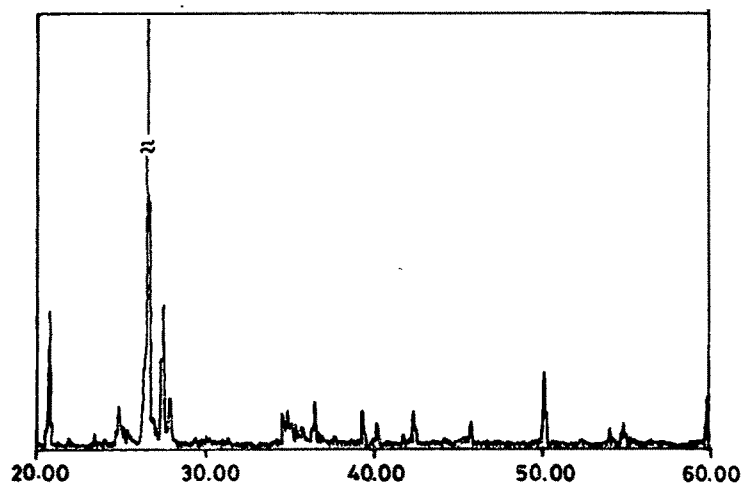
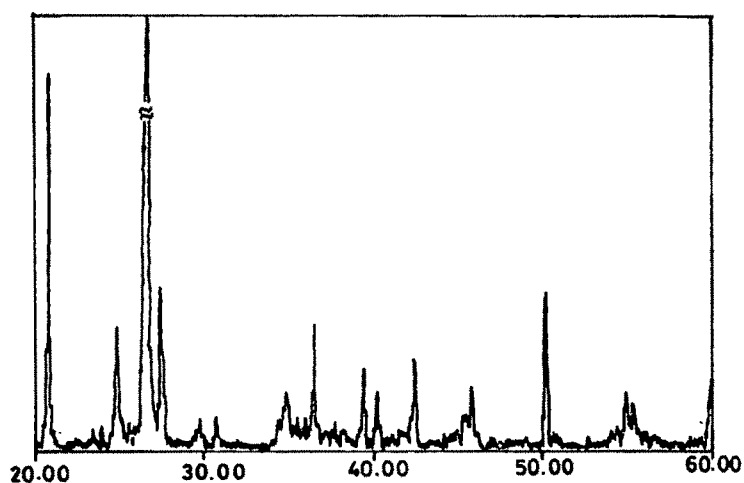


**TABLE 6.15 : XRD RESULTS OF SAMPLE C1/4 (KAMTHI).**

No.	2-THETA	d-spacing	I/I0	Minerals
1	20.830	4.261	22	Quartz
2	24.870	3.577	7	Microcline
3	26.610	3.347	100	Quartz
4	27.460	3.245	10	Microcline
5	30.770	2.903	2	Microcline
6	34.430	2.603	2	Sanidine
7	34.710	2.582	3	Sanidine
8	36.520	2.458	7	Quartz
9	39.440	2.283	5	Quartz
10	40.270	2.238	3	Quartz
11	42.410	2.130	6	Quartz
12	45.750	1.982	4	Quartz
13	50.110	1.819	10	Quartz
14	54.840	1.673	3	Quartz
15	55.300	1.660	2	Quartz
16	59.910	1.543	7	Quartz

**Fig. 6.12 : XRD Graph of sample C1/4.**



is conspicuously absent. Absence of K feldspar in Talchir clay (P<sub>4</sub>) and diamictite (P<sub>3</sub>) is because of their instability in a high pH environment which was prevailing during the deposition and subsequent lithification of Talchir sediments.

The mineral which shows very restricted development/presence in Lower Gondwana shales and clays is calcite. Its presence in substantial quantity in the Talchir diamictite or clay and their absence in Barakar, Barren Measures and Kamthi shale/clay point to their derivation from Pakhal rocks and subsequent recrystallization in an alkaline environment during the Talchir times.

Presence of clay minerals within the Lower Gondwana argillites was controlled by the Eh and ph of the interstitial fluids. As already discussed in thin section study, kaolinite formed in an humid, acidic and oxidising environment while chlorite formed in an arid, alkaline, and reducing climate. Change in the combination of these parameters can lead to the full or partial dissolution of one and crystallization of another. For example, occurrence of both kaolinite and chlorite and absence of calcite in the Talchir needle shale (P<sub>23</sub>) point to a mild acidic nature during the sedimentation of that unit. Similarly presence of chlorite and kaolinite in Barakar carbonaceous shale (P<sub>27</sub>) points to the fact that although the Eh condition, necessary for development of carbonaceous material, was reducing, the ph condition, that is generally associated with swampy conditions, was acidic. Thus within a single unit, presence of kaolinite or chlorite varies according to the type of existing groundwater chemistry although on a broad scale preponderance of one over another has imparted distinct colour to the rock-green, due to the abundance of chlorite and white, due to the abundance of kaolinite.

Notable occurrence of vermicullite within the Barakar clay is due to the alteration of biotite by introduction of water molecules in the biotite structure in a humid climate that was prevailing during the Barakar time.

Conspicuous presence of diopside (P<sub>4</sub>, P<sub>10</sub>, P<sub>23</sub>, C<sub>1/41</sub>) and phillipsite (P<sub>4</sub>, P<sub>27</sub>) point to the derivation of sediments from gabbro and anorthosite rocks occurring in the southeastern part of the basin (Please see provenance chapter). Presence of apatite (P<sub>3</sub>, C<sub>1/41</sub>) indicate a pegmatite source area.

Presence of siderite ( $P_{13}$ ) and hematite ( $P_4$ ,  $M_1/69$ ,  $M_1/58$ ) point to the concentration of Ferrous and Ferric iron in a reducing and oxidizing environment respectively.